Climate induced Congestion in Ports: General Equilibrium Consequences on Transportation and Trade

Jeanne Astier*

August 2025

Preliminary and Incomplete.
Please do not circulate.

Abstract

This paper studies the global impact of climate change effects on ports and its consequences on international trade, in the context of the shipping network. Leveraging detailed shipping and weather data, I estimate how sea weather shocks affect ports efficiency and transportation costs. I then include this effect in a model of international trade with a shipping network, featuring port congestion. This model can be used to estimate counterfactuals with climate change projections of sea weather: given the spatially heterogeneous evolution of weather shocks, I can quantify the global effects of climate change on transportation and trade through the port channel, as well as their spatial distribution.

Keywords: shipping, climate change, trade, weather

*Center for Research in Economics and Statistics (CREST), Institut Polytechnique de Paris. Email: jeanne.astier@ensae.fr.

1 Introduction

The impact of weather on economic outcomes has been widely documented for weather events happening on land through the channels of agriculture, productivity, capital. One important channel seems overlooked, although it is sensitive to weather conditions both on land and at sea: the transportation sector. Transportation is indeed essential for trade, and very sensitive to weather conditions – especially maritime transport. International trade is heavily relying on maritime freight: about 80% of traded goods are seaborne (UNCTAD, 2023). Yet, the shipping sector is often disrupted by weather events, especially those affecting port infrastructures.[1] Climate change is expected to worsen the weather conditions affecting ports, through sea-level rise and associated weather events (wind, waves, storm surge, coastal flooding...) (Pörtner et al., 2019). Such adverse weather translates into non-operability days for the ports, during which their activity is stopped or significantly reduced (Izaguirre et al., 2021). Their reduced capacity to receive ships might in turn cause congestion, resulting in increases of transportation costs (Brancaccio et al., 2024). Given the network structure of shipping (Heiland et al., 2019; Brancaccio et al., 2020; Ganapati et al., 2021), the effect of these local weather shocks could propagate to other ports and shipping routes, triggering a ripple effect with global consequences.

This project studies the global impact of climate change effects on ports and its consequences on international trade, in the context of the shipping network. I leverage detailed shipping and weather data to estimate how weather shocks affect ports efficiency, and hence transportation costs. I then include this effect in a model of international trade with a shipping network, featuring port congestion, based on Allen & Arkolakis (2022). This model can be used to estimate counterfactuals with projections of sea weather: given the evolution of weather shocks that will impact ports heterogeneously (Izaguirre et al., 2021), I can quantify the global effects on transportation and trade given the spillover mechanisms at play.

I rely on satellite automatic identification system (AIS) technology, a novel source of data inscreasingly used in the trade literature (Heiland et al., 2019; Brancaccio et al., 2020; Ganapati et al., 2021). I observe the exhaustive universe of port calls made by containerships in about 1,700 ports between 2015 and 2023, with their exact hour and date. These data allow to build measures of port efficiency, such as the port dwell time (the time ships spend in the port to be unloaded and reloaded) or the port incoming traffic (number of entering calls). I combine these measures with weather data at the location of the ports: I use wave height daily averages from the global reanalysis ERA-5 dataset (Hersbach et al., 2023), as a proxy for sea weather variables affecting ports. Reduced-form evidence shows that wave height significantly affects port efficiency: a jump from the 25th to the 75th percentile of daily average wave height increases the

[1] See for instance the closure of New York and New Jersey ports in October 2012 because of Hurricane Sandy, more recently the closure of Florida ports during hurricane Milton in October 2024.

dwell time by 2.5% and reduces the entering traffic by 7.9%. I find that this effect is non-linear and mostly driven by days with extreme wave height. The results also highlight spillovers: I construct port linkages using the shipping data, and find that a port's efficiency is affected not only by its own local wave height, but also by wave height in downstream ports.

To understand more precisely the spillover mechanisms and quantify global effects of weather shocks, I rely on a spatial economic model with optimal shipping route choice and endogenous traffic costs. I adapt the workhorse model of Allen & Arkolakis (2022), often used to study transportation between cities (e.g. Fuchs & Wong 2024), to an international trade and shipping setting. I consider that firms can export the goods they produce through ports, that are connected by a shipping network. To export from an origin to a destination, firms choose an optimal route that can go through several intermediate ports.[2] As opposed to the road network considered by Allen & Arkolakis (2022), I model congestion not on the *links* of the network but on the *nodes* – i.e. the ports: the cost of going through a port depends on the congestion in this port. Indeed, Brancaccio et al. (2024) show that a greater number of ships in a port forces ships to queue and hence increases the ships dwell time and service cost. I further assume that congestion in a port depends not only on the traffic if faces but also on the availability of its infrastructures, that can be affected by weather shocks. Using exact hat algebra techniques, I can then solve the model to determine the welfare effects of a counterfactual weather.

To quantify counterfactual scenarios, I need to estimate two key parameters: the elasticities of ships' dwell time to port congestion and to weather shocks. I leverage detailed AIS shipping data to estimate those, relying on a specification derived from the model – similarly to Fuchs & Wong (2024) but with an additional weather effect. I also propose a novel instrument for the endogenous traffic: since reduced-form evidence have highlighted the spillover effects of local weather shocks on port efficiency, I use weather shocks in downstream ports to instrument for a given port's traffic in a shift-share fashion. The estimates I obtain show that a 1% increase in port traffic raises ships dwell time by 0.6%, while +1 standard deviation (0.65m) in average wave height increases the dwell time by 1.6% – effects significant at the 1% level with a strong first stage.

Using these estimates and taking other structural parameters' values from the literature, I run a fixed point algorithm to solve for counterfactuals. I rely on country-level population and economic outcome from the World Penn Tables, and allocate those to ports by creating port catchment areas. There is indeed no one-to-one correspondence between ports and countries, as some countries are landlocked while others have multiple ports. I focus on the main 400 ports and define a catchment area for each, consisting of all regions for which this port is the closest

[2] Ganapati et al. (2021) highlight that most of shipping transportation is indirect, the goods stopping in several intermediate ports bewteen the origin and destination ports.

accessible option by road. Specifically, I start with a $0.25° \times 0.25°$ grid covering all countries, weighted by population (CIESIN, 2018), and assign each grid cell to its nearest port based on road distance (OpenRouteService, 2025), prioritizing domestic ports when available.

The first counterfactual scenario I consider is increasing the average wave height of each port one after the other, by 0.5m – a magnitude consistent with what the IPCC observed over the last decades (Pörtner et al., 2019). The results highlight the spillovers mechanisms: for instance, when shocking the weather in Singapore only, I find that the port of Singapore has decreasing traffic (-1.08%) and real income (-0.32%) – but other ports are also impacted: close ports also have decreasing traffic (for instance -0.5% in Port Kelang, Malaysia) as their trade flows with Singapore become more costly, but slightly increasing real outcome ($+0.06\%$ for Port Kelang) because the lower traffic reduces their congestion. Shocking ports one by one also allows to see which ports are the most critical for world welfare: isolated ports with a big catchment area have the highest global welfare elasticity – for instance, the port of Mombasa in Kenya.

The next step is to run counterfactuals shocking the weather in all ports simultaneously, relying on climate change weather projections (Pörtner et al., 2019). This work in progress will allow to quantify a global effect as well as the spatial distribution of local effects. I then would like to test the impact of local infrastructures mitigating the ports' vulnerability to weather (Christodoulou et al., 2019). This exercise could have policy implications in terms of which ports to protect in priority to maximize global welfare gains.

This project builds on the trade literature including transportation network. While this literature originally considers land transportation infrastructures at the country level, like highways or railroads (Fajgelbaum & Schaal, 2020; Allen & Arkolakis, 2022; Fuchs & Wong, 2024), an increasing body of works adapts these tools to study maritime transportation (Heiland et al., 2019; Brancaccio et al., 2020; Ganapati et al., 2021; Ludwig, 2024). I contribute to this literature by modeling further the specificities of the shipping network – in particular, displacing congestion from to *links* of the network to the *nodes*, based on the framework of Allen & Arkolakis (2022). This project also aims at studying transportation in an international context, rather than between cities of a same country: I further adapt the workorse model of Allen & Arkolakis (2014) to include specificities of international trade such as labor immobility and trade deficits between regions. I face the issue of non-isomorphism between the trading entities (countries) and transportation nodes (ports). While other papers in an international context consider only the country level, aggregating ports (Ganapati et al., 2021; Ludwig, 2024)[3], I try to provide a mapping between countries and ports by building port catchment areas.

[3]Which results in disregarding land-locked countries.

I also relate to the growing literature studying shipping from satellite AIS data. Most of this literature focuses on ships trips in a trade context (Heiland et al., 2019; Brancaccio et al., 2020; Ganapati et al., 2021), while a recent paper by Brancaccio et al. (2024) uses these data to study ports at the micro, country level. I try to connect these two approaches by including port congestion mechanisms identified by Brancaccio et al. (2024) in a global trade setting. The closest paper related to my work is Fuchs & Wong (2024), which studies a multi-modal transportation network including, among others, nodes congestion, also estimated using AIS data. My contribution with regard to this paper is to go from a country-level approach to a global setting and to propose a novel instrument for the estimation of congestion elasticity. I also propose to study a new mechanism which, to the best of my knowledge, has not been studied yet in this trade and shipping literature: the effect of weather shocks.

This weather shocks mechanism relates the paper to the environmental literature, first on the strand trying to quantifying the effect of climate change on economic outcomes. This impact has been widely documented for weather events happening on land – such as temperature shocks (Dell et al., 2012), hurricanes (Deryugina et al., 2018), floodings (Balboni et al., 2023), wildfires (Wang et al., 2021) ... – through channels like agriculture, productivity, capital. I propose to study sea weather shocks, focusing on wave height, and to uncover a new channel, the transportation sector. While some environmental works have been investigating the link between transportation and climate change, they mostly focus on how transportation contributes to climate change through emissions (see for instance Ludwig 2024 for the shipping sector). My perspective is rather to study how climate change related weather events can impact the transportation sector.

Finally, I also build on works studying in a reduced-form way the local impact of weather shocks on port operations (Becker et al., 2018; Christodoulou et al., 2019). I try to include these local effects in a global shipping framework, to include spillovers and quantify a global impact on economic outcome. I rely on the work of climate scientists Izaguirre et al. (2021) which provide evidence of the sea weather shocks affecting port operations and document the spatially heterogeneous effects that climate change will have on ports.

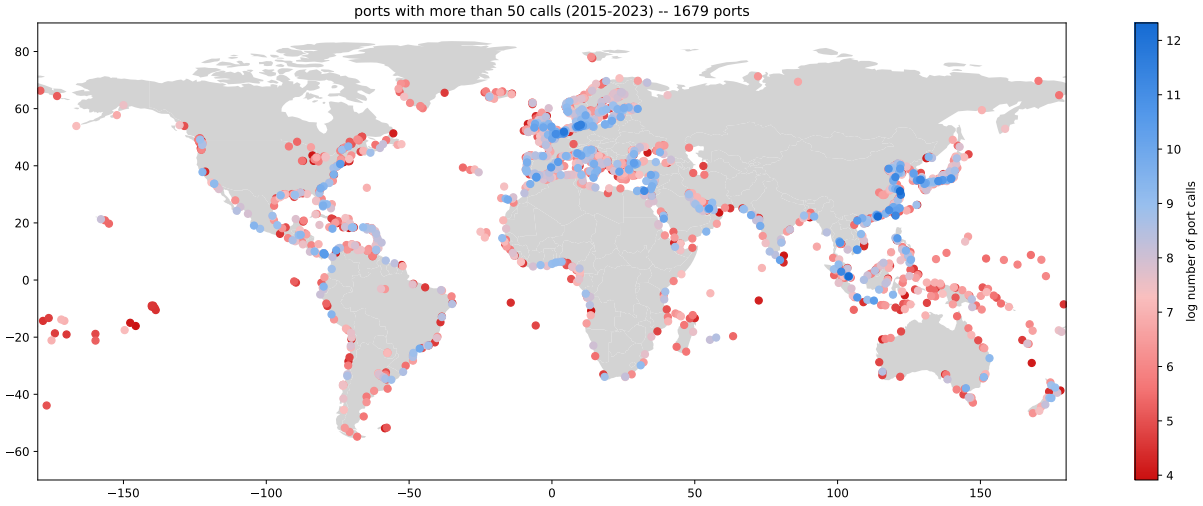
The rest of the paper is organized as follows. Section 2 presents the data used and provides reduced-form evidence of the effect of weather shocks on port efficiency. Section 3 details the economic geography model with shipping, based on Allen & Arkolakis (2022). I estimate the key parameters of this model in section 4. Finally, section 5 presents the counterfactual exercises and their results.

2 Data and Reduced-Form Evidence

2.1 Shipping and Weather Data

AIS shipping data I use shipping data based on satellite automatic identification system (AIS) technology, provided by Alphaliner. The dataset covers all containerships and their detailed port calls (i.e. anytime they enter or leave a port, with the exact position and time) between 2015 and 2023. I observe a large set of ports (around 1,700) all around the world, with varying traffic intensity, as the Figure 1 shows.

Figure 1: Ports observed in the shipping data, by traffic intensity (2015-2023)

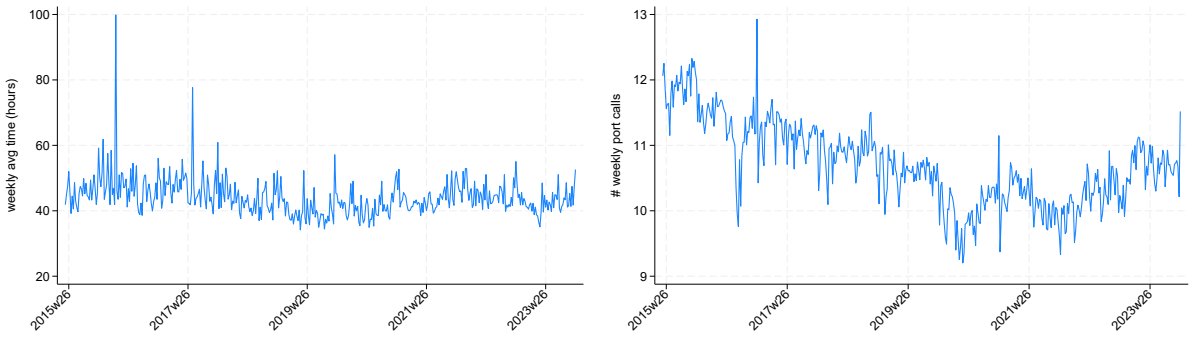


Note: The traffic intensity is computed as the logarithm of number of entering port calls over the total period.

For each port, I can use AIS shipping data to build two measures of port efficiency (Brancaccio et al., 2024). The port dwell time measures how long ships spend in the port (I compute it as their time of departure − time of arrival). It describes the time required by the port to unload and reload the ships, and hence measures the efficiency of port operations. The number of entering port calls measures the port traffic and its attractiveness. Figure 2 show descriptives of these two measures at the weekly frequency for the top 50 ports (in terms of traffic over the 2015-2023 period). It highlights the significant volatility in port efficiency. Summary statistics of efficiency measures for all ports are computed in Table B.1.

Sea weather data Port efficiency can be affected by various weather factors: wind strength and direction, wave height, storm surge, precipitation level... (Izaguirre et al., 2021). I use one weather variable as a proxy for global sea weather: the average daily wave height. While I am currently working on including a more exhaustive set of weather measures, this variable captures

Figure 2: Measures of efficiency for the top 50 ports observed in the shipping data (2015-2023)

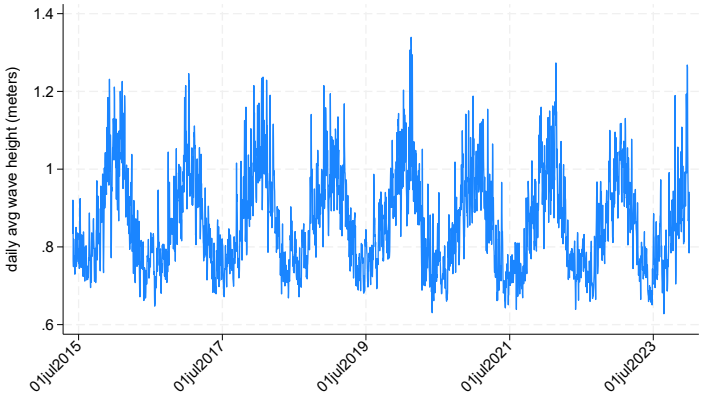


(a) Dwell time

(b) Number of entering calls

a significant effect, as reduced-form evidence shows below. I collect wave height daily averages from the global reanalysis ERA-5 dataset (Hersbach et al., 2023). I combine these gridded data at the 0.25°x 0.25° level with ports geographical positions, to get daily observations of port weather. Figure 3 shows the evolution of daily wave height over the period for the top 50 ports (in terms of traffic over the 2015-2023 period). It highlights the periodicity of wave height, which is higher (up to 1.2m) around December and lower (down to 0.7m) around June. There is also significant volatility bewteen days. Summary statistics of wave height for all ports are computed in Table B.2.

Figure 3: Average daily wave height in the top 50 ports observed in the shipping data (2015-2023)



2.2 Reduced-Form Evidence: Effect of Weather Shocks on Port Efficiency

I combine shipping data with wave height observations, to produce evidence of weather impact on port efficiency. I first provide evidence of the direct effect of a port's own local weather shocks on

its efficiency, then highlight spillover mechanisms between the different ports connected through the shipping network.

Direct effect of local shocks I test the effect of a port's wave height on its efficiency with the following specification:

$$y_{it} = \alpha + \beta \text{ weather}_{it} + \delta_i + \delta_t + \epsilon_{it} \tag{1}$$

where y_{it} is a measure of port i efficiency during day t (log average dwell time or total number of entering calls), weather_{it} is the weather at port i during day t (average significant wave height). δ_i is a port fixed-effect, δ_t a day fixed effect; in alternative specifications, I include other fixed-effects such as port-month or country-day. When y_{it} is the number of port calls, I estimate a Poisson model. Standard errors are clustered at the port or at the country level.

Results in Table 1 show a significant effect of daily wave height of port efficiency: +1m of wave height (which is equal to around 1.5 standard deviation) increases the dwell time by 2 to 3% and reduces the number of entering calls by 10 to 11%. These effects are robust across the different sets of fixed effects included and level of clusterisation of the standard errors.

Table 1: Effect of wave height average on port efficiency (daily)

	(1)	(2)	(3)	(4)
	log time	# calls	log time	# calls
wave	0.0329***	-0.1009***	0.0207***	-0.1160***
	(0.0028)	(0.0051)	(0.0042)	(0.0150)
date (day) FE	✓	✓		
port FE	✓	✓		
port-month FE			✓	✓
country-day FE			✓	✓
SE cluster level	port	port	country	country
# observations	2,024,333	5,223,201	1,818,036	4,134,980
# clusters	1,679	1,679	128	132

Standard errors in parentheses

* $p < 0.10$, ** $p < 0.05$, *** $p < 0.01$

Instead of measuring weather as the average daily wave height, I can also build bins of daily wave height, to capture potential non-linear effects. For each port, I build percentiles of wave height over the period (2015-2023), and then measure the effect of a day where the wave height is either below the median, between the median and the 90th percentile, between the 90th percentile and the 99th percentile, above the 99th percentile. Results in Table 2 show that the effects of

wave height on port efficiency are indeed non-linear: compared to a day where wave height is below the median, a day where wave height higher than the 99th percentile has a much higher effect than a day where the wave height is between the 90th and 99th percentiles, for instance. The effect of local weather shocks on a ports' efficiency thus seems to be driven by extreme events.

Table 2: Effect of wave height bins on port efficiency (daily)

	(1) log time	(2) # calls	(3) log time	(4) # calls
wave <p50	*ref*	*ref*	*ref*	*ref*
wave p50-p90	0.0121***	-0.0153***	0.0045**	-0.0127***
	(0.0016)	(0.0016)	(0.0018)	(0.0028)
wave p90-p99	0.0288***	-0.0965***	0.0136***	-0.0890***
	(0.0035)	(0.0052)	(0.0035)	(0.0155)
wave >p99	0.0735***	-0.4467***	0.0460***	-0.4171***
	(0.0090)	(0.0302)	(0.0117)	(0.0861)
date (day) FE	✓	✓		
port FE	✓	✓		
port-month FE			✓	✓
country-day FE			✓	✓
SE cluster level	port	port	country	country
# observations	2,024,333	5,223,201	1,818,036	4,134,980
# clusters	1,679	1,679	128	132

Standard errors in parentheses

* $p < 0.10$, ** $p < 0.05$, *** $p < 0.01$

In appendix C.1, I show in an event-study setting that weather shocks also have an effect before and after the exact moment they actually happen. Port efficiency is indeed reduced not only on the day when it experiences extreme waves, but also during the days before and after. This suggests that the daily effects observed above might only been a lower bound of the total weather effect.

Appendix C.2 performs similar reduced-form exercises but at the *ship* level, rather than aggregating by port. The results are consistent, a higher wave height in a port increasing the dwell time of all ships entering into this port.

In appendix C.3, I additionally show that weather *inside* a port might have an effect on ships behavior *outside* of ports: when a port is disrupted, ships might prefer to wait outside of the port

(to avoid paying additional port fees). I indeed find that high wave height in origin or departure port increase the trip duration of ships. This suggests once again that the effects observed in the ports might be only a lower bound of the full effects, since they do not capture ships waiting outside of ports.

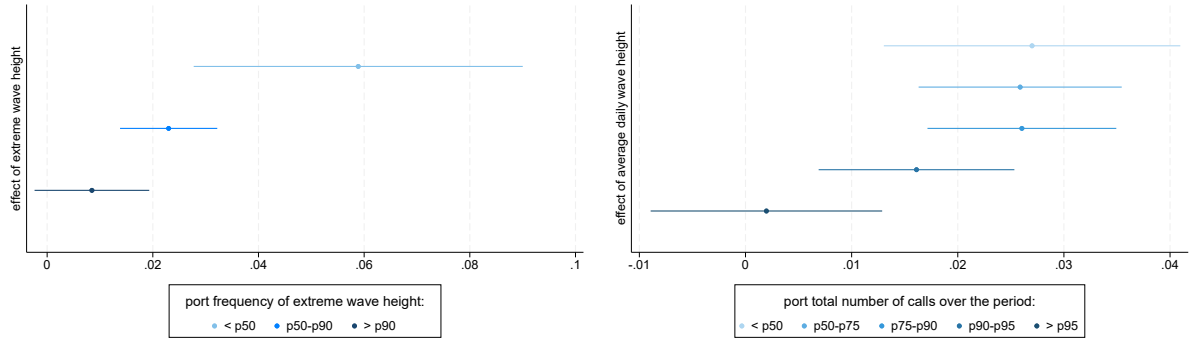
An important consideration is why weather conditions in ports warrant greater analytical emphasis than those encountered at sea during the transit between ports. While it is true that vessels typically spend a larger share of their voyage at sea – where they may be exposed to adverse phenomena such as storms, high waves, and strong winds – maritime navigation allows for considerable flexibility. In particular, vessels can adjust their course in response to meteorological forecasts, a practice commonly referred to as weather routing. In contrast, ports are geographically fixed and thus more vulnerable to local weather disruptions. In addition, the adverse effects of weather shocks in ports are amplified by infrastructure constraints leading to congestion, while the open sea is unconstrained by physical infrastructure. To empirically assess the differential importance of weather conditions in ports versus those along the maritime route, I conduct a comparative analysis of their effects on shipping duration in Appendix C.4. The results indicate that adverse weather in ports has a more pronounced effect on shipping times, as it influences both port dwell times and the duration of journeys between ports.

Heterogeneity analysis There is potential heterogeneity in the reactions of ports to weather shocks. I investigate this heterogeneity along two dimensions: the exposure of ports to adverse weather conditions and the size of ports.

I measure port exposure to adverse weather conditions as the number of days during the period (2015-2023) where the daily wave height of a port is greater than 1.7m (the 90th percentile of daily wave height). I then divide the sample of 1,679 ports into three sub-samples: the ports with a number of high wave days below the median; between the median and the 90th percentile; above the 90th percentile. For each subsample, I regress the average daily dwell time of ports on a dummy indicating whether the wave height is extreme (>1.7m) during this day, with date, port-month, and country-year fixed effects. Standard errors are clustered at the port level. The results are displayed in the left panel of Figure 4: the magnitude of the effect is decreasing with frequency of exposure. For ports of the first group, which are rarely exposed to extreme wave height, a day with extreme wave height increases dwell time by about 6% compared to a day with normal wave height; this effect is no more statistically different from 0 for the ports that experience the most frequently such wave heights. This suggests an adaptation behavior of ports: as the frequency of adverse weather events increases, ports could adapt their process and infrastructure to mitigate the negative impact on their efficiency.

The heterogeneity along port size goes in the same direction. I measure port size as the total

Figure 4: Heterogeneous effects of wave height on ports



(a) by port exposure to extreme wave height

(b) by port size

number of entering calls in each port over the period (2015-2023). I then divide the sample of 1,679 ports into 5 sub-samples: the ports with a number of calls below the median; between the median and the 75th percentile; between 75th and the 90th percentile; between 90th and the 95th percentile; above the 95th percentile.[4] For each subsample, I then regress the average daily dwell time on average daily wave height, with date, port-month, and country-year fixed effects. Standard errors are clustered at the port level. The results are displayed in the right panel of Figure 4: the magnitude of the effect is decreasing with port size – mostly for very big ports. Indeed, all ports below the 90th percentile of traffic have similar effects of daily wave height, increasing dwell time by around 2.7%; this effect falls to practically 0 for the biggest 5% of ports. The biggest ports are likely to be the ones with the most developed infrastructures, confirming the narrative of infrastructures as a mitigation device.

Spillover effects Because the ports are connected through a shipping network (Heiland et al., 2019; Brancaccio et al., 2020; Ganapati et al., 2021), the efficiency of a port might be affected not only by its own weather but also by the weather of upstream and downstream ports. I observe the network connecting ports in the shipping data: for a port of interest, I build a weighting scheme accounting for the importance of other ports based on containership trips. I distinguish between downstream and upstream network shocks, depending on whether they hit ports that are respectively after or before of the port of interest in the ships trips. Formally, I consider that

[4]With extreme weather events, a power issue prevents from dividing the sample into too many sub-samples, as I study the effect of an extreme event which frequency is used to create the sub-samples. This issue is less important when dividing along port size as ports of all sizes are exposed to adverse weather.

a given port i at time t can be hit by downstream and upstream shocks defined as follows:

$$\text{weather}_{it}^{\text{Down}} = \sum_j \omega_{ij}^D \text{ weather}_{jt} \tag{2}$$

$$\text{weather}_{it}^{\text{Up}} = \sum_j \omega_{ij}^U \text{ weather}_{jt} \tag{3}$$

where weather_{jt} is the direct weather shock hitting port j at date t: I take a weighted average of the shocks hitting all ports j that port i has a linkage with. I construct the weights from the containership trips over the whole period (2015-2023). From the perspective of port i, I build the weights for downstream shocks as the ratio of the number of containerships going to port j from port i, over the total number of containerships leaving from port i:

$$\omega_{ij}^D = \frac{\text{flows}_{i \to j}}{\sum_k \text{flows}_{i \to k}} \tag{4}$$

The weights associated with measures of upstream shocks are constructed as the ratio of the number of containerships going from port j to port i, over the total number of containerships coming to port i:

$$\omega_{ij}^U = \frac{\text{flows}_{j \to i}}{\sum_k \text{flows}_{k \to i}} \tag{5}$$

The flows might be endogenous to weather, for instance if ships re-reroute and change origin or destination port when there is bad weather in one of these ports. To avoid this endogeneity, when computing the weights I restrict the flows considered. For downstream weights, I consider only the flows that happen when none of the origin port or any of the destination port it is related to, are subject to extreme weather (defined as waves greater than the 95th percentile at that port over the period). For upstream weights, I consider only the flows that happen when none of the destination port or any of the origin port it is related to, are subject to extreme weather. Doing so, I should avoid having weights influenced by weather conditions.

I finally estimate the following econometric specification:

$$y_{it} = \beta \text{ weather}_{it} + \gamma^{\text{Down}} \text{ weather}_{it}^{\text{Down}} + \gamma^{\text{Up}} \text{ weather}_{it}^{\text{Up}} + \delta_i + \delta_t + \epsilon_{it} \tag{6}$$

The estimated (standardized) coefficients in Table 3 show that port efficiency is significantly affected by downstream weather shocks. Wave height in downstream ports has effects of the same sign as the local wave height: it increases the dwell time and reduces the number of calls – the magnitude being about twice lower. The mechanisms could come from re-rerouting decisions: when there is adverse weather in the next ports, ships might adapt and change their decisions of port or adapt their timing. These findings point toward the importance of weather shocks

spillovers through the shipping network.

Table 3: Effect of local, upstream and downstream wave height (standardized)

	(1) log time	(2) # calls
Local wave height	0.0172***	-0.0518***
	(0.0022)	(0.0040)
Downstream wave height	0.0075***	-0.0289***
	(0.0025)	(0.0046)
Upstream wave height	-0.0022	0.0061*
	(0.0026)	(0.0032)
port FE	✓	✓
day FE	✓	✓
# observations	1,987,500	4,340,499
# ports	1,398	1,398

Standardized coefficients

Standard errors (clustered by port) in parentheses

* $p < 0.10$, ** $p < 0.05$, *** $p < 0.01$

3 Economic Geography Model with Shipping

The reduced-form evidence shows that port efficiency is affected by weather shocks, and that these effects propagate through the shipping network. To understand better the spillovers mechanism and estimate the global effect of weather shocks, I use an economic geography model of trade with shipping. I rely on the workhorse model of Allen & Arkolakis (2022) (A&A henceforth), designed to study road or rail transportation between cities, and adapt it to an international trade and shipping setting. I present the model below, highlighting the differences from A&A. In the presentation of the model, I abstract from time subscripts t for clarity, but I consider that this static model can be repeated over time.

3.1 Model set up

Consider a finite number of countries $c \in \{1, ..., C\} \equiv \mathcal{C}$, inhabited by $\bar{L}$ individuals, and a finite number of ports $i \in \{1, ..., N\} \equiv \mathcal{N}$ $(N > C)$.[5] The ports are located in countries – countries can have between zero and several ports. The countries are populated by individuals (resp. firms), who can locate in different regions of the country; they are related to the closest port of their

[5] In the original A&A model, there is an isomorphism between regions c and transport nodes i are they consider cities. Here, I introduce the distinction between the two as I am considering trade between countries but transportation between ports.

region from which they can import and consume (resp. produce and export) goods. Each port thus has a catchment area where are located individuals and firms related to this port. Let $\omega_{c,i}$ denote the share of individuals and firms of country c that belong to port i catchment area.

Ports $i \in \mathcal{N}$ are connected by a transportation (shipping) network, represented by two matrices:

- as in A&A, a $N \times N$ matrix of links costs $\mathbf{T} = [t_{kl} \geq 1]$, where t_{kl} is the ad valorem (iceberg) cost incurred from moving directly from $k \in \mathcal{N}$ to $l \in \mathcal{N}$ along a link (if there is no link, then $t_{kl} = +\infty$).
- an additional $N \times 1$ matrix of nodes costs $\mathbf{P} = [p_k \geq 1]$, where p_k is the ad valorem cost incurred from going through port $k \in \mathcal{N}$.

Goods move from an origin port i to a destination port j through a route r, defined as a sequence of links and intermediate nodes connecting i to j. A route of length K from i to j is a sequence of $K+1$ locations and the links in between: $r \equiv \{r_0 = i, r_1, ..., r_K = j\}$. Since iceberg costs are multiplicative, the total cost of route r is

$$p_i \times t_{i,k_1} \times p_{k_1} \times t_{k_1,k_2} \times ... \times t_{k_{K-1},j} \times p_j = \underbrace{\left(\prod_{l=0}^{K} p_{r_l}\right)}_{\text{cost of nodes}} \underbrace{\left(\prod_{l=1}^{K} t_{r_{l-1},r_l}\right)}_{\text{cost of links}} \tag{7}$$

There are multiple routes going from origin i to destination j: let $\mathcal{R}_{ij}$ denote their set.

Goods are traded across port catchment areas (also referred to as locations). In this international setting, labor is considered to be immobile between locations.[6] Each individual related to port catchment area $i \in \mathcal{N}$ supplies one unit of labor inelastically (labor being the only factor of production) for a wage w_i. Individuals also purchase quantities of a continuum of goods $\nu \in [0, 1]$ with constant elasticity of substitution σ. Let Y^W denote the total income in the economy. In what follows, average per capita income is taken as the numeraire: $Y^W/\bar{L} = 1$.

Each location $i \in \mathcal{N}$ is endowed with a constant return to scale technology for producing and shipping each good $\nu \in [0, 1]$ to each destination $j \in \mathcal{N}$ along each route $r \in \mathcal{R}_{ij}$. The technology is origin-destination-route specific, subject to idiosyncratic shocks $\epsilon_{ij,r}(\nu)$ – following Eaton & Kortum (2002), $\epsilon_{ij,r}(\nu)$ is independently and identically Fréchet-distributed across routes and goods, with a scale parameter $1/\bar{A}_i$ (capturing origin-specific efficiency) and a shape parameter θ (regulating the shock dispersion).

[6] As opposed to A&A setting that considers cities within a country, where labor is perfectly mobile.

Under perfect competition, the price in destination j of a good sourced in origin i and shippped along route r is given by

$$p_{ij,r}(\nu) = w_i \frac{\left(\prod_{l=0}^{K} p_{r_l}\right)\left(\prod_{k=1}^{K} t_{r_{k-1},r_k}\right)}{\epsilon_{ij,r}(\nu)} \tag{8}$$

Individuals in location j purchase each good $\nu \in [0,1]$ from the cheapest source (i.e. origin-route).

3.2 Gravity and equilibrium

Following closely A&A, given the Fréchet distribution of origin-destination-route specific productivities, the probability that $j \in \mathcal{N}$ purchases good $\nu \in [0,1]$ from $i \in \mathcal{N}$ along route $r \in \mathcal{R}_{ij}$ can be written as:

$$\pi_{ij,r} = \frac{\left(w_i/\bar{A}_i\right)^{-\theta}\left(\prod_{l=0}^{K} p_{r_l}^{-\theta}\right)\left(\prod_{l=1}^{K} t_{r_{l-1},r_l}^{-\theta}\right)}{\sum_{k\in\mathcal{N}}\left(w_k/A_k\right)^{-\theta}\sum_{r'\in\mathcal{R}_{kj}}\left(\prod_{l=0}^{K} p_{r'_l}^{-\theta}\right)\left(\prod_{l=1}^{K} t_{r'_{l-1},r'_l}^{-\theta}\right)} \tag{9}$$

The total value of goods shipped from i to j, X_{ij} is obtained by summing across all routes r connecting i to j. As in Eaton & Kortum (2002), the probability of purchasing a good is equal to the expenditure share, yielding

$$X_{ij} = \sum_{r\in\mathcal{R}_{ij}} \pi_{ij,r} E_j = \frac{(w_i/\bar{A}_i)^{-\theta}\tau_{ij}^{-\theta}}{\sum_{k\in\mathcal{N}}(w_k/\bar{A}_k)^{-\theta}\tau_{kj}^{-\theta}} E_j \tag{10}$$

where τ_{ij} is the transportation cost from i to j – with an additional nodes cost term compared to A&A:

$$\tau_{ij} \equiv \left(\sum_{r\in\mathcal{R}_{ij}}\left(\prod_{l=0}^{K} p_{r_l}^{-\theta}\right)\left(\prod_{l=1}^{K} t_{r_{l-1},r_l}^{-\theta}\right)\right)^{-\frac{1}{\theta}} \tag{11}$$

Market clears at the equilibrium: total income Y_i in each location is equal to its total sales, and total expenditure E_i is each location is equal to its total purchases:

$$Y_i = \sum_{j=1}^{N} X_{ij}\ , \quad E_i = \sum_{j=1}^{N} X_{ji}, \tag{12}$$

Under these conditions, one can then retrieve the usual gravity equation:

$$X_{ij} = \tau_{ij}^{-\theta} \times \frac{Y_i}{\Pi_i^{-\theta}} \times \frac{E_j}{P_j^{-\theta}} \tag{13}$$

where Π_i and P_j are the market access terms (or multilateral resistance terms) as in Anderson & Van Wincoop (2003). Π_i is a producer price index capturing the (inverse) producer market access, while P_j is the consumer price index capturing the (inverse) consumer market access terms:

$$\Pi_i \equiv \left(\sum_j \tau_{ij}^{-\theta} E_j P_j^{\theta} \right)^{-\frac{1}{\theta}}, \quad P_j \equiv \left(\sum_i \tau_{ij}^{-\theta} Y_i \Pi_i^{\theta} \right)^{-\frac{1}{\theta}} \tag{14}$$

I introduce the same notations as A&A and define $y_i \equiv Y_i / Y^W$ and $l_i \equiv L_i / \bar{L}$ as the share of total income and total labor in location $i \in \mathcal{N}$, respectively. As opposed to A&A, labor is immobile: l_i is thus exogenously determined ($l_i = \bar{l}_i$) and there is no equalization of welfare across locations.

In this international trade setting, I assume that trade is imbalanced:[7] denoting D_i the deficit, $E_i = Y_i + D_i$ (with $\sum_i D_i = 0$). I further assume that the deficit is a share of local outcome, as in Costinot & Rodríguez-Clare (2014): $D_i = \kappa_i Y_i$. Hence

$$E_i = (1 + \kappa_i) Y_i \tag{15}$$

Combining these equations[8], I obtain the following equilibrium conditions:

$$\bar{A}_i^{-\theta} \bar{l}_i^{-\theta} y_i^{1+\theta} = \sum_j \tau_{ij}^{-\theta} (1 + \kappa_j) y_j P_j^{\theta} \tag{16}$$

$$P_i^{-\theta} = \sum_j \tau_{ji}^{-\theta} \bar{A}_j^{\theta} \bar{l}_j^{\theta} y_j^{-(\theta+1)} \tag{17}$$

Given $\{\bar{A}_i\}$, $\{\bar{l}_i\}$, $\{\tau_{ij}\}$, $\{\kappa_i\}$, 16 and 17 constitute a system of $2N$ equations can be solved to get equilibrium $\{y_i\}$ and $\{P_i\}$. However, similarly to A&A, I want to make the transportation costs endogenous, through traffic congestion, so that they also respond to the equilibrium distribution of y_i and P_i.

3.3 Endogenous transportation costs and weather

The first step is to write an analytical relationship between (i) transportation network characterized by links and nodes costs t_{ij} and p_i, and (ii) transportation costs τ_{ij}. I follow and adapt A&A procedure: starting from $\tau_{ij}^{-\theta} = \sum_{r \in \mathcal{R}_{ij}} \left(\prod_{l=0}^{K} p_{r_l}^{-\theta} \right) \left(\prod_{l=1}^{K} t_{r_{l-1}, r_l}^{-\theta} \right)$ (equation 11)

[7] A&A consider balanced trade between cities; however in international trade data, expenditures are not equal to income, i.e. countries operate either in surplus or in deficit in a given year.

[8] See Appendix A.1 for detailed derivation of the equilibrium conditions.

and enumerating all possible routes,[9] it comes that

$$\tau_{ij}^{-\theta} = \sum_{K=0}^{+\infty} (\mathbf{D}^K)_{ij}\, p_i^{-\theta}$$

where $\mathbf{D}$ is the $N \times N$ matrix of general term $d_{ij} \equiv t_{ij}^{-\theta} p_j^{-\theta}$, and $(\mathbf{D}^K)_{ij}$ is the term of the i-th and j-th column of matrix $\mathbf{D}$ to the power K. Provided that the spectral radius of $\mathbf{D}$ is less than one, the geometric sum can be expressed as:

$$\sum_{K=0}^{+\infty} \mathbf{D}^K = (\mathbf{I} - \mathbf{D})^{-1} \equiv \mathbf{C}^D$$

where $\mathbf{C}^D = \left[c_{ij}^D\right]$ is the Leontief inverse of the $\mathbf{D}$ matrix. As a result, the transportation cost from i to j can be written as a function of the transportation network:

$$\tau_{ij}^{-\theta} = c_{ij}^D\, p_i^{-\theta} \tag{18}$$

Once there is an analytical relationship between transportation network and transportation costs, the next step is to make the transportation network depend on traffic. Adapting A&A setting from *links* to *nodes*, I characterize the expected number of times in which a node k is used in trade between i and j, π_{ij}^k:

$$\pi_{ij}^k = \sum_{r \in \mathcal{R}_{ij}} \left(\frac{\pi_{ij,r}}{\sum_{r' \in \mathcal{R}_{ij}} \pi_{ij,r'}} \right) n_r^k \tag{19}$$

which can be rewritten as:[10]

$$\pi_{ij}^k = \frac{\tau_{ik}^{-\theta}\, p_k^{\theta}\, \tau_{kj}^{-\theta}}{\tau_{ij}^{\theta}} \tag{20}$$

This equation is close to Allen & Arkolakis (2022) as I can isolate a cost on the left of the node, the cost of the node, a cost on the right of the node. The third term of the equation might be confusing because of the positive exponent on p_k: this is because p_k already enters (negatively) in both τ_{ik} and τ_{kj}, so it is double counted.

Let Ξ_k be the node traffic in location k, i.e. the value of all goods going through node k (either because they have k as an origin or destination, or just because they transit through k as an intermediate node along their route):

$$\Xi_k = \sum_{i \in \mathcal{N}} \sum_{j \in \mathcal{N}} \pi_{ij}^k X_{ij} \tag{21}$$

[9] See Appendix A.2 for detailed derivation of the analytical relationship between τ_{ij}, t_{ij} and p_i.
[10] See Appendix A.3 for detailed derivation of traffic expressions.

This expression can be written as gravity equation for node traffic, with the same market access terms as a the gravity equation for trade flows 13:

$$\Xi_k = p_k^{\theta} \times P_k^{-\theta} \times \Pi_k^{-\theta} \tag{22}$$

A&A also show that similarly, link traffic Ξ_{kl} can be expressed with a gravity equation for link traffic:

$$\pi_{ij}^{kl} = \frac{\tau_{ik}^{-\theta}\ t_{kl}^{-\theta}\ \tau_{lj}^{-\theta}}{\tau_{ij}^{\theta}} \tag{23}$$

$$\Xi_{kl} = t_{kl}^{-\theta} \times P_k^{-\theta} \times \Pi_l^{-\theta} \tag{24}$$

With (i) the analytical relationship between transportation cost τ_{ij} and network costs t_{ij}, p_i given by 18, and (ii) expressions of traffic given by 22 and 24, I can now introduce congestion by making the network costs t_{ij}, p_i depend on traffic – which will ultimately impact transportation cost τ_{ij}. Differently from A&A, to better represent shipping transportation (while they focus on railroads or highway transportation) I do not introduce traffic congestion on the *links* but rather on the *nodes* of the transportation network. I assume that the direct cost of traveling over a link is exogenously given (for instance by the distance of the link):

$$t_{kl} = \bar{t}_{kl} \tag{25}$$

The cost of traveling through a node will however depend in this node's traffic. More precisely, I follow Brancaccio et al. (2024) in assuming that the cost of going through a port depends on the amount of time spent on this port:[11]

$$p_k = (\text{time}_k)^{\delta_0} \tag{26}$$

where time_k is the dwell time at port k and δ_0 is the time elasticity of the transportation cost. The time spent in a port depends in turn on the port's capacity and traffic:[12]

$$\text{time}_k = \omega_k \left(\frac{\Xi_k}{K_k}\right)^{\delta_1} \tag{27}$$

[11] Brancaccio et al. (2024) show that the cost for a ship to stop in a port has a fixed amount (for port services) and an additional amount depending on the time spent in the port. Their descriptive statistics show that the time-depending part constitutes the majority of the total cost. They also notice that their estimate of time cost might be a lower bound as it only includes the cost of staying in the port, but not delays for the next transportation step nor the inventory costs that importers and exporters face. Relying on this, I neglect the fixed part of port cost to focus only on the time-depending part. Additionally, Brancaccio et al. (2024) show evidence of a convex relationship between time at port and traffic, which justifies the functional form in equation 26.

[12] This functional form is a simplification compared to Brancaccio et al. (2024) who assume that time $= T\left(1 + \mathbb{1}\{Q > K\}\frac{Q-K+1}{K}\right)$ where T the service time (depending on productivity of the port, labor, number of cranes...), Q the number of ships queuing, K the port capacity. In equation 27 I abstract from the distinction between the time ships spend queuing and being unloaded/reloaded.

where ω_k is the productivity of port k (capturing for instance the labor force, productivity shocks...) and K_k the port capacity (number of ships that can be handled simultaneously, e.g. related to the number of berths). δ_1 is the congestion elasticity of time spent at port. Finally, the port capacity is affected by weather conditions:

$$K_k = \exp(\gamma \text{ weather}_k)\ \delta_k \tag{28}$$

where weather_k is a measure of weather at port k and δ_k captures other components of port capacity. Combining equations 26, 27 and 28 yields

$$p_k = \omega_k^{\delta_0} \delta_k^{-\delta_0\delta_1} \exp(-\gamma\delta_0\delta_1 \text{ weather}_k)(\Xi_k)^{\delta_0\delta_1} \quad \text{i.e.} \quad p_k = \bar{\Gamma}_k \exp(\mu \text{ weather}_k)(\Xi_k)^{\lambda} \tag{29}$$

$\bar{\boldsymbol{T}} = [\bar{t}_{kl}]$ and $\bar{\boldsymbol{\Gamma}} = \left[\bar{\Gamma}_k\right]$ describe the infrastructure network, exogenously given. $\lambda = \delta_0\delta_1 > 0$ is the congestion elasticity, $\mu = -\gamma\delta_0\delta_1 > 0$ is the weather elasticity. Equation 29 is similar to the endogenous link cost equation of A&A: the transportation cost endogenously depends on traffic – the key difference in my setting being that the congestion elasticity λ plays a role on the *nodes* cost (rather than the *links*). Fuchs & Wong (2024) also include node congestion in their model, in a similar fashion. The additional weather elasticity μ is a novelty compared to both Allen & Arkolakis (2022) and Fuchs & Wong (2024).

Combining equation 29 with the gravity equation for node traffic 22 yields

$$p_k = \bar{\Gamma}_k^{\frac{1}{1-\lambda\theta}}\ e^{\frac{\mu}{1-\lambda\theta}\ \text{weather}_k}\ P_k^{\frac{-\lambda\theta}{1-\lambda\theta}}\ \Pi_k^{\frac{-\lambda\theta}{1-\lambda\theta}} \tag{30}$$

3.4 General equilibrium and exact hat algebra

Combining the equilibrium expressions 16 and 17 with equations 18, 24 and 30 allows to write the general equilibrium of the model with endogenous port costs.[13] Given a local geography $\{\bar{A}_i, \bar{l}_i\}_{i\in\mathcal{N}}$, an aggregate labor endowment $\bar{L}$, trade deficits $\{\kappa_i\}_{i\in\mathcal{N}}$, an infrastructure network $\bar{\mathbf{T}} = [\bar{t}_{kl}]$ and $\bar{\boldsymbol{\Gamma}} = [\bar{\Gamma}_k]$, a weather measure $\{\text{weather}_i\}_{i\in\mathcal{N}}$ and model parameters $\{\theta, \lambda, \mu\}$, the equilibrium is a distribution of economic activity $\{y_i, P_i\}_{i\in\mathcal{N}}$ satisfying:

$$\begin{aligned} y_i^{\theta+1+\frac{\lambda\theta(\theta+1)}{1-\lambda\theta}} P_i^{-\frac{\lambda\theta^2}{1-\lambda\theta}} =& \bar{L}^{-\frac{\lambda\theta}{1-\lambda\theta}} \bar{A}_i^{\frac{\lambda\theta^2}{1-\lambda\theta}+\theta} \bar{\Gamma}_i^{\frac{-\theta}{1-\lambda\theta}} e^{\frac{-\mu\theta}{1-\lambda\theta}\text{weather}_i} \bar{l}_i^{\frac{\lambda\theta^2}{1-\lambda\theta}+\theta} (1+\kappa_i) y_i P_i^{\theta} \\ &+ \bar{L}^{-\frac{\lambda\theta}{1-\lambda\theta}} \sum_{j=1}^{N} \bar{A}_i^{\frac{\lambda\theta^2}{1-\lambda\theta}+\theta} \bar{A}_j \bar{t}_{ij}^{-\theta} \bar{\Gamma}_i^{\frac{-\theta}{1-\lambda\theta}} e^{\frac{-\mu\theta}{1-\lambda\theta}\text{weather}_i} \bar{l}_i^{\frac{\lambda\theta^2}{1-\lambda\theta}+\theta} \bar{l}_j^{-\theta} y_j^{1+\theta} \end{aligned} \tag{31}$$

[13] See Appendix A.5 for detailed derivation of the equilibrium equations.

$$
\begin{aligned}
y_i^{\frac{\lambda\theta(\theta+1)}{1-\lambda\theta}} P_i^{-\theta-\frac{\lambda\theta^2}{1-\lambda\theta}} =& \bar{L}^{\frac{-\lambda\theta}{1-\lambda\theta}} \bar{A}_i^{\frac{\lambda\theta^2}{1-\lambda\theta}+\theta} \bar{\Gamma}_i^{\frac{-\theta}{1-\lambda\theta}} e^{\frac{-\mu\theta}{1-\lambda\theta}\text{weather}_i} \bar{l}_i^{\frac{\lambda\theta^2}{1-\lambda\theta}+\theta} y_i^{-\theta+1} \\
&+ \bar{L}^{-\frac{\lambda\theta}{1-\lambda\theta}} \sum_{j=1}^{N} \bar{A}_i^{\frac{\lambda\theta^2}{1-\lambda\theta}} \bar{t}_{ij}^{-\theta} \bar{\Gamma}_i^{\frac{-\theta}{1-\lambda\theta}} e^{\frac{-\mu\theta}{1-\lambda\theta}\text{weather}_i} \bar{l}_i^{\frac{\lambda\theta^2}{1-\lambda\theta}} P_j^{-\theta}
\end{aligned} \tag{32}
$$

To quantify the impact of a weather shock affecting ports infrastructure, I rely on the standard exact hat algebra approach and write the model in terms for changes from the equilibrium – using the notations $\hat{x}_i \equiv \frac{x_i'}{x_i}$ and $\Delta x_i \equiv x_i' - x_i$.

Consider a change in weather $\{\Delta\text{weather}_i\}_{i\in\mathcal{N}}$ and a change in trade deficits $\{\widehat{(1+\kappa_i)}\}_{i\in\mathcal{N}}$[14]. Given observed link traffic flows $\{\Xi_{ij}\}$, economic activity $\{Y_i, E_i\}$, and model parameters $\{\theta, \lambda, \mu\}$, the equilibrium change in economic outcomes $\{\hat{y}_i, \hat{P}_i\}$ is the solution of the following system of equations:[15]

$$
\begin{aligned}
\hat{y}_i^{\frac{1+\theta}{1-\lambda\theta}} \hat{P}_i^{\frac{-\theta}{1-\lambda\theta}+\theta} =& \left(\frac{E_i}{E_i + \sum_j \Xi_{ij}}\right) e^{\frac{-\mu\theta}{1-\lambda\theta}\Delta\text{weather}_i} \widehat{(1+\kappa_i)} \hat{y}_i \hat{P}_i^{\theta} \\
&+ \sum_{j=1}^{N} \left(\frac{\Xi_{ij}}{E_i + \sum_j \Xi_{ij}}\right) e^{\frac{-\mu\theta}{1-\lambda\theta}\Delta\text{weather}_i} \hat{y}_j^{\theta+1}
\end{aligned} \tag{33}
$$

$$
\begin{aligned}
\hat{y}_i^{\frac{\theta+1}{1-\lambda\theta}-(\theta+1)} \hat{P}_i^{\frac{-\theta}{1-\lambda\theta}} =& \left(\frac{Y_i}{Y_i + \sum_j \Xi_{ji}}\right) e^{\frac{-\mu\theta}{1-\lambda\theta}\Delta\text{weather}_i} \hat{y}_i^{-\theta} \\
&+ \sum_{j=1}^{N} \left(\frac{\Xi_{ji}}{Y_i + \sum_j \Xi_{ji}}\right) e^{\frac{-\mu\theta}{1-\lambda\theta}\Delta\text{weather}_i} \hat{P}_j^{-\theta}
\end{aligned} \tag{34}
$$

4 Estimation: Congestion and Weather Elasticities

There are two key elasticities to estimate to take to model to the data: the congestion elasticity and the weather elasticity. I can derive an estimation equation for them from the model microfoundations and take it to the shipping and weather data described above. Combining equations 27 and 28 leads to

$$
\text{time}_i = \Xi_i^{\delta_1} e^{-\delta_1\gamma\ \text{weather}_i} \omega_i^{\delta_1} \delta_i \tag{35}
$$

Building on Fuchs & Wong (2024), I consider the following estimation equation:

$$
\ln(\text{time}_{sit}) = \delta_1 \ln(\Xi_{i,[t-X;\,t]}) - \delta_1\beta\ \text{weather}_{it} + \delta_{si} + \delta_t + \delta_{iy} + \epsilon_{sit} \tag{36}
$$

where s denotes a ship, i a port, t a day and y a year. time_{sit} is the dwell time experienced

[14] With a slight abuse of notation: $\widehat{(1+\kappa_i)} = \frac{1+\kappa_i'}{1+\kappa_i}$

[15] See Appendix A.6 for detailed derivation of the exact hat algebra equilibrium equations.

by ship s in port i on day t. $\Xi_{i,[t-X;\,t]}$ is a moving average of traffic at port i over the X days before t. I consider traffic over the past days to capture the potentially long-lasting effects of congestion – since it is increasing the dwell time, it might propagate to the next days. Similarly, $\text{weather}_{i,[t-X;\,t]}$ is a moving average of weather at port i over the X days before t. I also consider weather over the past days for several reasons: 1/ reduced-form evidence have shown that weather shocks can have effects lasting after the actual event (Figure C.1); 2/ since weather also affects dwell time indirectly through traffic (that is endogenous and depends on port costs, hence on local weather) and that I consider traffic over the past days, I also need to control for weather over this period. I add ship-port, port-year and day fixed-effects. The standard errors are two-way clustered at the ship and port levels. I set X = 14 days, but I find similar results using a longer time period for the moving averages (especially setting X = 28 as Fuchs & Wong 2024 do).

The measure of weather used in the estimation must reflect the key insights from the reduced-form evidence. I include two variables. First, we have seen that effect of wave height on port efficiency is non-linear and driven by extreme events (Table 2). To account for this, I use the share of days of the period where the port experiences extreme wave height (above 2.5m[16]):

$$\text{weather}^1_{i,[t-X;\,t]} = \{\text{share days} > 2.5\text{m}\}_{i,[t-X;\,t]}$$

Second, reduced-form heterogeneity results have shown that there is adaptation to the effect of extreme waves when they become more frequent (Figure 4). To account for this, I rely on Carleton et al. (2022) and interact short the run weather variable weather^1 with a long-run climate variable, the sample-period average wave height:

$$\text{weather}^2_{i,[t-X;\,t]} = \{\text{share days} > 2.5\text{m}\}_{i,[t-X;\,t]} \times \{\text{avg wave height}\}_i$$

I expect the coefficient of weather^1 to be positive, as bad weather increases port dwell time, but the coefficient of weather^2 to be negative as a higher long-run average wave height means that the port is likely more adapted to bad weather.

The measure of port traffic Ξ_{it} is defined as the number of ships present at the port i during day t, weighted by the share of the day the ships spend at the port[17] and by the ships capacity (vessel dead-weight tonnage).

There is an endogeneity issue with port traffic $\Xi_{i,[t-X;\,t]}$. The main threat to identification comes from potential reverse causality if the traffic is influenced by the time spent in port – for instance, when the dwell time begins to increase, ships might start to avoid the port, reducing

[16] This value is defined by Izaguirre et al. (2021) as a threshold above which port activity is severely disrupted.

[17] e.g. if a ship arrives very late in the day, it will not contribute as much to traffic this as a ship arrived very early in the day

traffic. Additionally, the unobserved shocks in the error term might affect both traffic and dwell time (productivity shocks for instance). I propose a novel instrument, compared to Fuchs & Wong (2024): reduced-form evidence have shown that the efficiency of a port is impacted not only by its own weather, but also by the weather of other ports, especially downstream (Table 3). I hence build a shift-share instrument where the weights are based on port-interlinkages observed in shipping data; and the shifts are wave height variations in other ports. More precisely, the instrument is defined as follows:

$$\mathbf{Z}_{i,[t-X;\,t]} = \sum_{s} \omega^{D}_{is} \mathbf{weather}_{s,[t-X;\,t]} \tag{37}$$

where $\mathbf{weather}_{s,[t-X;\,t]}$ is a moving average of wave height measures (daily average and bins) over the past X (14 here) days in port s, and ω^{D}_{is} is defined in equation 4.

To be valid, this instrument needs to be relevant and exogenous. Relevance (i.e. $\mathbf{Z}$ correlated with Ξ) has been shown in the reduced-form evidence: adverse weather in downstream ports tends to change the efficiency of an upstream port – hence influencing its congestion. When a downstream port is congested, ships might anticipate and take rerouting decisions affecting their stay in upstream ports. Exogeneity requires that $\mathbf{Z}$ is correlated with the dwell time solely through its correlation with congestion Ξ. This seems plausible in the setting considered: the time ships spend in a port depends on congestion in this port, not on other endogenous factors – especially not on a decision: ships cannot decide to stay longer in a port if the next one is congested. This assumption is realistic as staying in a port is costly, hence ships would no prefer to stay in an upstream port longer than required – they would rather wait *outside* of the port than stay longer in a port.[18]

Results are reported in Table 4. I consider three specifications: including only weather among the regressors (columns 1 and 2), including also traffic but not instrumenting for it (columns 3 and 4), finally implementing the IV strategy (columns 5 and 6). For each specification, I include for weather either only the measure of extreme wave height, or also the interaction with long-run wave height average to account for adaptation. The coefficients of weather elasticity have the expected signs: bad weather reduces port efficiency, but this negative effect is mitigated when the long-run climate is worse thanks to adaptation. The OLS estimator of traffic elasticity is very close to the one of Fuchs & Wong (2024) (I find 0.14 while there OLS estimate is 0.10), although I also include weather, consider a shorter moving average window and a more exhaustive set of ports. The instrument used in the IV specification is almost sufficiently strong, as the heteroskedasticity-robust Kleibergen-Paap rk Wald F statistic (KP-F) is very close to 10[19].

[18] Table D.7 shows that downstream weather has no effect on port dwell time when controlling for port traffic.

[19] In an alternative specification with different weather measures, I find a stronger instrument (KP-F $>$ 10) and similar traffic elasticity, see Table D.9.

Table 4: Effect of moving-average traffic and weather on port dwell time

	no traffic		OLS		IV	
	(1)	(2)	(3)	(4)	(5)	(6)
% days ≤2.5m (MA)	*ref*	*ref*	*ref*	*ref*	*ref*	*ref*
% days >2.5m (MA)	0.13415***	0.36019***	0.12051***	0.32141***	0.06558***	0.18666**
	(0.01524)	(0.04751)	(0.01267)	(0.03924)	(0.01999)	(0.07990)
% days >2.5m (MA) × avg wave height		-0.15519***		-0.13794***		-0.07855*
		(0.02962)		(0.02510)		(0.04566)
log traffic (MA)			0.13972***	0.13960***	0.69811***	0.63017***
			(0.00586)	(0.00586)	(0.09775)	(0.09270)
date FE	✓	✓	✓	✓	✓	✓
ship-port FE	✓	✓	✓	✓	✓	✓
port-year FE	✓	✓	✓	✓	✓	✓
# observations	6,710,321	6,710,321	6,710,224	6,710,224	6,710,224	6,710,224
# ships	11,557	11,557	11,557	11,557	11,557	11,557
# ports	1,357	1,357	1,357	1,357	1,357	1,357
First Stage KP-F					9.230	9.259
First Stage CD-F					701.1	696.0

Standard errors in parentheses

* $p < 0.10$, ** $p < 0.05$, *** $p < 0.01$

The IV value of traffic elasticity is higher than the one found by Fuchs & Wong (2024) using a different instrument (they find a value of 0.25). For taking the model to the data, I rely on the elasticities of specification 6, highlighted in the Table 4.

Table D.8 in Appendix shows the results using another instrument for traffic: I use traffic at the same date one year before, to instrument for traffic at a given date. This allows in particular to get rid of the potential reverse causality issue. I find similar results with an instrumented congestion elasticity of higher magnitude than the un-instrumented one, though lower than in Table D.9 (0.24 rather than 0.59, which is closer to Fuchs & Wong (2024) estimate).

5 Shipping Network Weather Shocks

I now turn to counterfactuals. I first explain how I take the model to the data, then present the results of counterfactual exercises where I shock the weather of each port one after another.

5.1 Taking the model to the data

Structural parameters The estimation presented below allows to recover values of δ_1 and γ, related respectively to the congestion and weather elasticities. I turn to the literature to get values of other structural parameters. I rely on Allen & Arkolakis (2022) for the value of θ: I take $\theta = 8$ from Donaldson & Hornbeck (2016). I follow the same approach as Fuchs & Wong (2024) to set a value for δ_0, relying on Hummels & Schaur (2013): from their level-log elasticity

of trade costs to transportation time, I derive a log-log elasticity of 0.4. Table 5 summarizes the parameters values used to compute the counterfactuals.

Table 5: Structural parameters values used in the counterfactuals computation

parameter	value	source
θ	8	Donaldson & Hornbeck (2016)
δ_0	0.4	Fuchs & Wong (2024); Hummels & Schaur (2013)
δ_1	0.6	estimation
λ	0.24	$\delta_0\delta_1$
γ^1, γ^2	$-0.30, 0.12$	estimation
μ_1, μ_2	$0.08, -0.03$	$-\gamma^1\delta_0\delta_1, -\gamma^2\delta_0\delta_1$

Port catchment areas I consider the top 400 container ports[20] and define their respective catchment areas. To do so, I start with a 0.25° × 0.25° grid (representing cells of up to 30 km × 30 km at the Equator) covering all countries, weighted by population (CIESIN, 2018). Each grid cell is then assigned to the most relevant port based on the following rules:

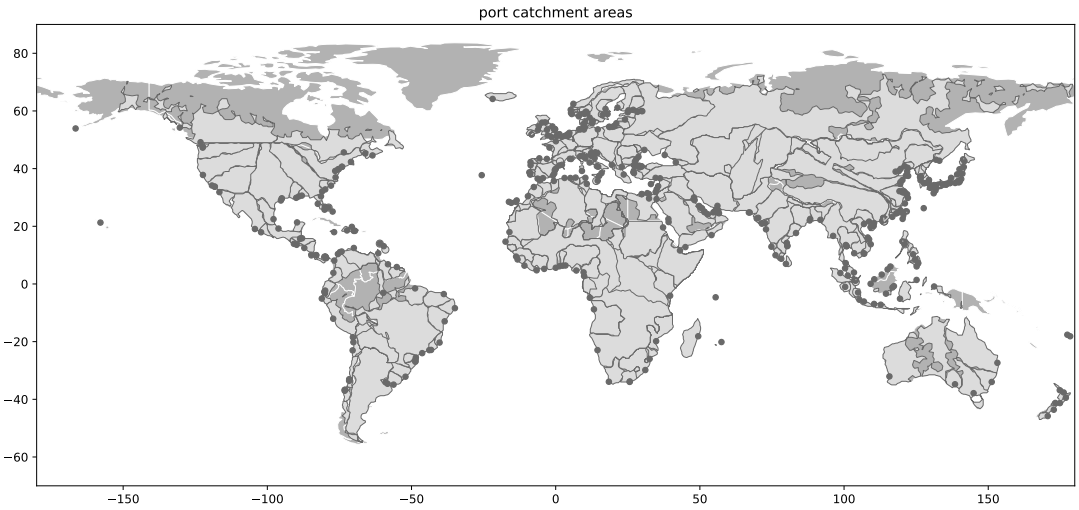
1. if the country has ports, the cell is allocated to the closest domestic port;
2. if the country is landlocked, the cell is allocated to the closest land-accessible foreign port.

These rules reflect a preference for domestic ports, even when a foreign port may be geographically closer. Distances are computed using the Open Route Service API (OpenRouteService, 2025), which accounts for actual road networks rather than straight-line ("as-the-crow-flies") distances. This adjustment is crucial, especially in developing countries where sparse or indirect road networks can significantly increase travel distances. Additionally, I incorporate port importance into the catchment area calculation. Larger and better-equipped ports may attract more exports and imports, even when farther away. To account for this, I use total entering port calls over the 2015–2023 period as a proxy for port importance and adjust distances accordingly. Specifically, I scale the road distance to each port by $1/\sqrt{\text{port importance}}$. This formulation implies that if two ports are at the same location but one is twice as large as the other, its catchment area will be twice as extensive.[21] With this procedure, I compute port catchment areas, i.e. shares of land related to each port, plotted in Figure 5. A port catchment area can cover only a part of a country (e.g. French ports cover each one a share of French territory), a whole country or even several countries (e.g. the port of Calcutta catchment area covers part of India but also Nepal and Bhutan).

[20] The raw AIS data contain many ports that are not adapted for containerships, or that are in fact technical stops for ships (for fuel, maintenance...) but not ports, etc. I use a cleaned version of the dataset to only look at point identified as container ports.

[21] For example, without adjusting for port importance, I find that only 1% of Chinese exports would go through Shanghai, despite it being the world's largest port, because it is located in a region with many other ports. Incorporating port importance corrects for this distortion.

Figure 5: Port catchment areas worldwide



Note: Ports are plotted as dark dots, and port catchment areas are plotted as gray areas delimited by dark lines. The catchment area of a given port is the area in which this port is located. Parts of the world belong to no port catchment area because they have no road network to connect them to ports (e.g. the Amazon rainforest).

Outcome, expenditure, and traffic From the port catchment areas, I can compute the population-weighted shares of each country c related to each port i, $\omega_{c,i}$. I then rely on Penn World Tables to get country-level outcome Y_c and expenditure E_c for the year 2019. From these, I build port-level outcome $Y_i = \sum_c \omega_{c,i} Y_c$, representing the amount of goods produced by firms that export through port i (that can come from different countries); and port-level expenditure $E_i = \sum_c \omega_{c,i} E_c$, representing the amount of goods consumed by agents that import through port i (coming from potentially different countries as well).

To solve the exact hat algebra system of equations 33 and 33, I additionally require to observe traffic flows Ξ_{ij}. I take them from AIS shipping data, considering the shipping links that have more than 50 calls over the year 2019, between the 400 ports I take into account. For these links, I measure traffic Ξ_{ij} as the number of ships (weighted by their capacity) traveling on the link during the year 2019.

Treatment effects With these data and structural parameters values, I can compute the treatment effects of a given weather shock $\{\Delta\text{weather}_i\}_{i\in\mathcal{N}}$ following the exact hat algebra system of equations 33 and 34. I take trade deficits into account using a two-step procedure (Ossa, 2016). I first compute counterfactual outcomes assuming no weather shock but taking the trade deficits to zero; then I compute counterfactuals with a weather change assuming the trade deficits stay to zero. The treatment effect of the change in weather is computed as the difference between

equilibrium levels in the two counterfactuals. This procedure is detailed in Appendix F. To solve the system of equations, I use a fixed point algorithm (adapted from the one of Allen & Arkolakis 2022, see Appendix G).

I retrieve the equilibrium changes in nominal economic outcome $\{\hat{y}_i\}_{i\in\mathcal{N}}$ and price index $\{\hat{P}_i\}_{i\in\mathcal{N}}$ at the port catchment area level, from which I can derive changes in real outcome $\{\hat{y}_i/\hat{P}_i\}_{i\in\mathcal{N}}$ – the reference welfare metric used by Arkolakis et al. (2012). To better understand the mechanisms leading to these welfare effects, I also look at the changes in port traffic $\{\hat{\Xi}_i\}_{i\in\mathcal{N}}$ and route traffic $\{\hat{\Xi}_{ij}\}_{i,j\in\mathcal{N}}$.

I can also aggregate these effects at the country level, either exactly for changes in nominal outcome $\{\hat{y}_c\}_{c\in\mathcal{C}}$ or using average as a proxy for changes in real outcome $\{\hat{y}_c/\hat{P}_c\}_{c\in\mathcal{C}}$:[22]

$$y_c = \sum_{i\in\mathcal{N}} \omega_{c,i}\, y_i \;\Rightarrow\; \hat{y}_c = \frac{\sum_{i\in\mathcal{N}} \omega_{c,i}\, y_i \hat{y}_i}{\sum_{i\in\mathcal{N}} \omega_{c,i}\, y_i} \qquad \text{and} \qquad \text{proxy}(\frac{\hat{y}_c}{\hat{P}_c}) = \sum_i \omega_{c,i} \frac{\hat{y}_i}{\hat{P}_i} \tag{38}$$

Similarly, global change of nominal income at the world level can be easily computed as

$$y = \sum_{i\in\mathcal{N}} y_i \qquad \Rightarrow \qquad \hat{y} = \frac{\sum_{i\in\mathcal{N}} y_i \hat{y}_i}{\sum_{i\in\mathcal{N}} y_i} \tag{39}$$

And I can compute global average change in real outcome, weighted by nominal outcome or by population, as a proxy for global welfare:

$$\frac{\sum_{i\in\mathcal{N}} y_i\, (\hat{y}_i/\hat{p}_i)}{\sum_{i\in\mathcal{N}} y_i} \qquad \text{and} \qquad \frac{\sum_{i\in\mathcal{N}} l_i\, (\hat{y}_i/\hat{p}_i)}{\sum_{i\in\mathcal{N}} l_i} \tag{40}$$

5.2 Predicted vs observed trade flows

As in Allen & Arkolakis (2022), there is a close link in the model between the gravity equation for trade flows (equation 13) and the gravity equation of traffic on links (equation 24). Combining these equations allows to write an expression of equilibrium trade flows as:[23]

$$X_{ij} = Y_i \times c_{ij}^X \times E_j \tag{41}$$

where c_{ij}^X is the (i,j)-th element of the matrix $\mathbf{C^X} \equiv \left(\mathbf{D^X} - [\Xi_{ij}]\right)^{-1}$, where $\mathbf{D^X}$ is a diagonal matrix with i-th element equal to $d_i^X \equiv \frac{1}{2}\left(Y_i + E_i\right) + \frac{1}{2}\left(\sum_j \Xi_{ij} + \Xi_{ji}\right)$.

[22] I cannot compute the exact change in real outcome at the country level since I do not observe the baseline price levels. I can however compute the country-level average change in real outcome as a proxy. This proxy gives a sense of the average welfare change at the country level.

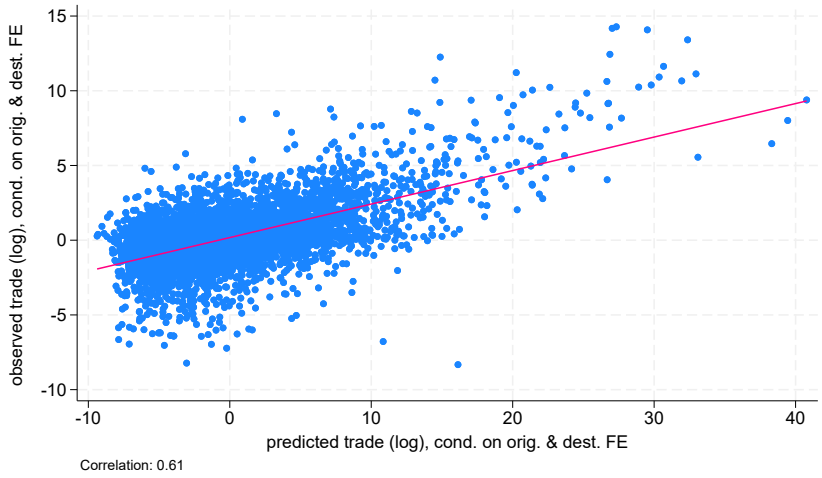
[23] See Appendix A.4 for detailed derivation of the relationship between trade flows and traffic flows.

Following Allen & Arkolakis (2022), this expression for traffic flows between locations i and j depends only on available data. It allows to build a *prediction* of trade flows based on the model, that we can then compare with *observed* trade flows from data, to check the validity of the model.

I rely on traffic flows between ports which catchment area does not cover several countries. From the traffic flows Ξ_{ij}, the outcome Y_i and expenditure E_i of those ports, I can predict trade flows at the *port level* X_{ij} using equation 41. I then aggregate ports to the country they belong to, to get predicted trade flows of the *country level* $X_{c,c'}$. I compare these model-precicted trade flows with bilateral trade flows data at the country level from Mayer et al. (2023) and Fontagné et al. (2023) in 2019 (aggregating all manufacturing and agriculture sectors together).[24]

Figure 6 shows the scatter plot between observed and predicted log trade flows, conditional on origin and destination fixed effects.[25] The strong positive correlation (0.61) indicates that the traffic matrix is efficient in predicting the trade flows. This suggests the model is performing well to describe international trade flows with a shipping network, extending the result of Allen & Arkolakis (2022) showing that their original model performs well to describe trade between cities in US with a road network.

Figure 6: Predicted trade flows using traffic compared to observed trade flows



[24] Mayer et al. (2023) and Fontagné et al. (2023) combine data on annual cross-border international bilateral flows (UN Commodity Trade Statistics Database (COMTRADE) for manufacturing and Food and Agriculture Organization of the United Nations Statistics Division (FAOSTAT) for agriculture) with production data (the UNIDO Industrial Statistics database (INDSTAT) for manufacturing and again FAOSTAT for agriculture) to compile a square matrix of bilateral trade flows for each sector, including self-trade.

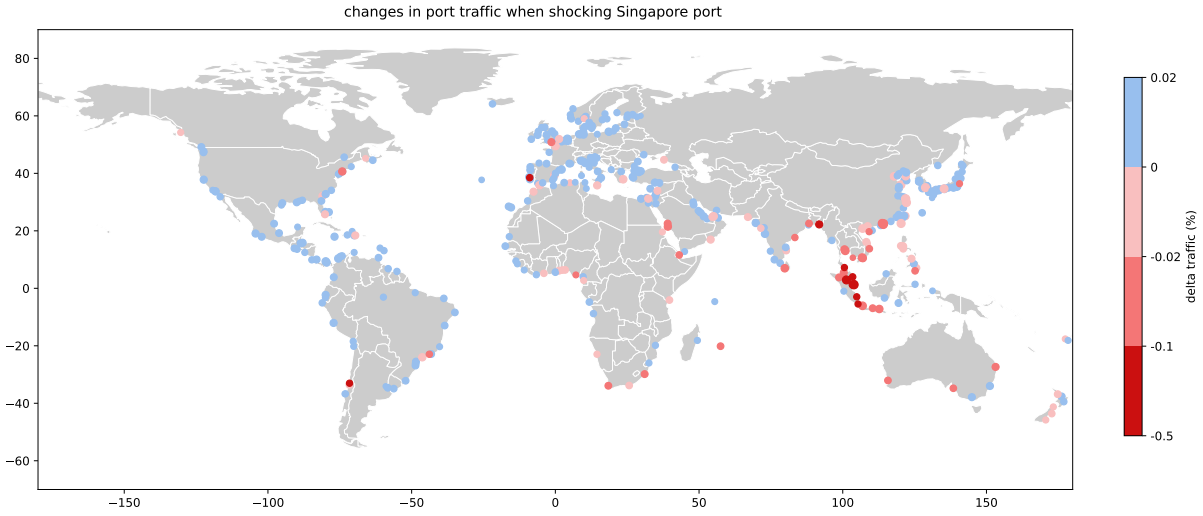
[25] As Allen & Arkolakis (2022) notice, controlling for origin country and destination fixed effects allows that the variation arises only from the bilateral flows and not from characteristics of origin or destination countries such as income. See Figure E.3 for a comparison of observed and predicted log trade flows, unconditional on origin and destination fixed effects: the correlation is lower but still strongly positive (0.54), with a similar magnitude to what A&A find.

5.3 Counterfactuals: marginal shocks effects

I look at the effects of shocking weather in one unique port. The shock is an increase of 6 percentage points in the share of days with waves higher than 2.5m, and an increase of 50cm in average wave height. Those values correspond to the standard errors observed in the data and they are consistent with the magnitude described by the IPCC over the past decades (Pörtner et al., 2019). I present below the results of one particular port shock, Singapore, to illustrate the spillovers mechanisms at play. I then show the effect on global welfare of each port shock. Counterfactuals when shocking all ports simultaneously according to climate changes scenarios are work in progress.

Shocking Singapore port Looking first at the effect on port traffic (Figure 7), I find as expected that the most impacted port is Singapore (−0.5% of traffic). The closest ports are negatively affected as well, there is for instance decreasing traffic in ports of Pasir Gudang and Port Kelang (−0.3%) in Malaysia. This can be explained by the fact that those close ports have important traffic flows to/from Singapore, so the increased port cost in Singapore affects their traffic. As the distance from Singapore increases, the effect on port traffic becomes positive and gets bigger, although of lower magnitude – up to +0.01% for ports in West Africa and Northern America. There is also slightly increasing traffic in a few ports close to Singapore (e.g. +0.02% in Padang and in Bitung, in Indonesia), illustrating the traffic flows substitution at play.

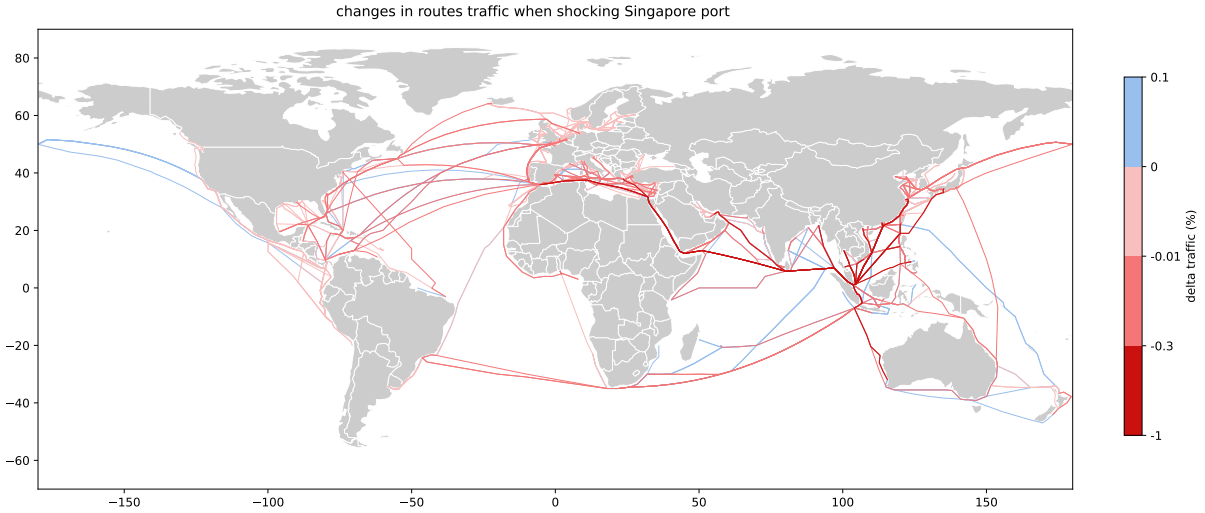
Figure 7: Changes in port traffic when increasing wave height in Singapore



Turning to the effects on routes traffic (Figure 8), I find that the most impacted links are the ones related to Singapore – for instance Singapore-Nansha or Singapore-Shanghai (−1%). This is caused by higher transportation costs along these links. Quite the opposite, the highest increases in traffic happen along the routes in the Singapore region but not directly connected

to Singapore – for instance Chittagong-Port Kelang or Belawan-Tanjung Pelepas (+0.1%).

Figure 8: Changes in route traffic when increasing wave height in Singapore



In terms of real outcome changes $\hat{y}_i/\hat{P}_i$ (i.e. welfare changes, Arkolakis et al. 2012)[26] at the port catchment level (Figure 9), the most impacted region is once again Singapore itself (−0.32% of real outcome). The closest regions have slightly increasing welfare (+0.06% for the region of Pasir Gudang in Malaysia, +0.04% for the port catchment area of Chittagong in Bangladesh). Other regions of the world are impacted with very little magnitude. Regions very far away very slightly increase their real outcome (e.g. up to +0.004% in USA or Norther Europe port catchment areas), while intermediate regions (nor too close nor too far) experience a slight decrease (e.g. up to −0.003% in Piraeus, Greece).

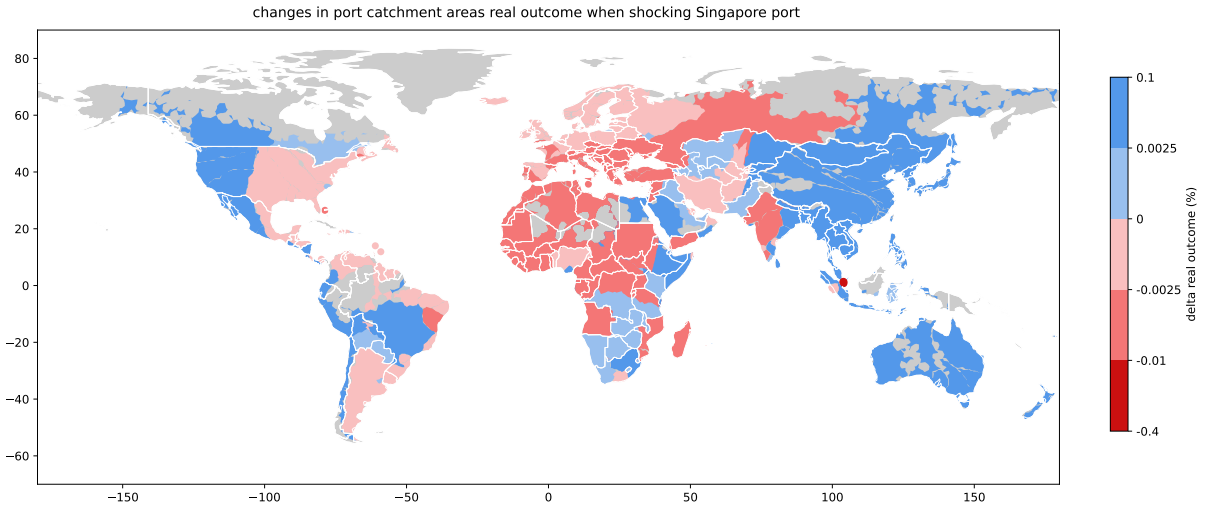
The pattern is very similar when considering changes at the country scale (Figures H.5 and H.6).

Global welfare elasticity of each port For each port, I can see how the global average real outcome evolves after an increase of wave height in this single port. Figure 10 shows these effects using population-weighted average real outcome (see equation 40) as a proxy for global welfare.[27] The majority of ports have a negative effect on global welfare when being shocked. The ports that have the biggest impact are Mombasa in Kenya (−0.1% of global welfare), Mundra in India, (−0.05%), Lagos in Nigeria (−0.02%). Those ports are not the biggest ones but they are impactful as they have quite and very populated catchment areas, and they are in addition isolated

[26] The *real outcome* changes exacerbate the patterns displayed by the *nominal outcome* changes $\hat{y}_i$, presented in Figure H.4.

[27] See Figures H.7 and H.8 in Appendix for the effect on global nominal outcome and global income-weighted average real outcome.

Figure 9: Changes in real outcome at the port catchment area level when increasing wave height in Singapore



(not many possible substitution ports around).

The correlation matrix displayed in Figure 11 helps study the characteristics leading some ports to be more critical than others for global welfare. As expected, the effect on global welfare of a shock in a port seems very negatively correlated with the population and outcome of its catchment area. However, the proximity to other ports[28] does not seem to be very correlated with the size of the global welfare elasticity.

It is worth noticing that several ports have a very slightly positive effect on world welfare when being hit: these are big ports, located in very dense areas — like Port Kelang in Malaysia (+0.004%), Singapore (+0.004%)... This effect is rather surprising, even though it has a very small magnitude. It might be driven by the congestion externalities present in the model: because of them, some of the ports are too busy compared to what an optimal planner would have set. Shocks in such ports force reallocation of traffic and partly correct for these externalities by reallocating some traffic of the busiest ports to their neighbor ports.

The magnitude of the effects found in the counterfactual analyses might seem very small – at most -0.1% of global welfare; but these are effects when shocking *only one single port*. Climate change counterfactual scenarios, which are work in progress, will consist of weather shocks in *all ports simultaneously*, which will lead to significantly more important effects.

[28] Measured as a proximity index, defined as the average of inverse distance of each other port. The distance to other ports can be scaled by the size of these other ports.

Figure 10: Population-weighted global real outcome changes when increasing wave height in each port

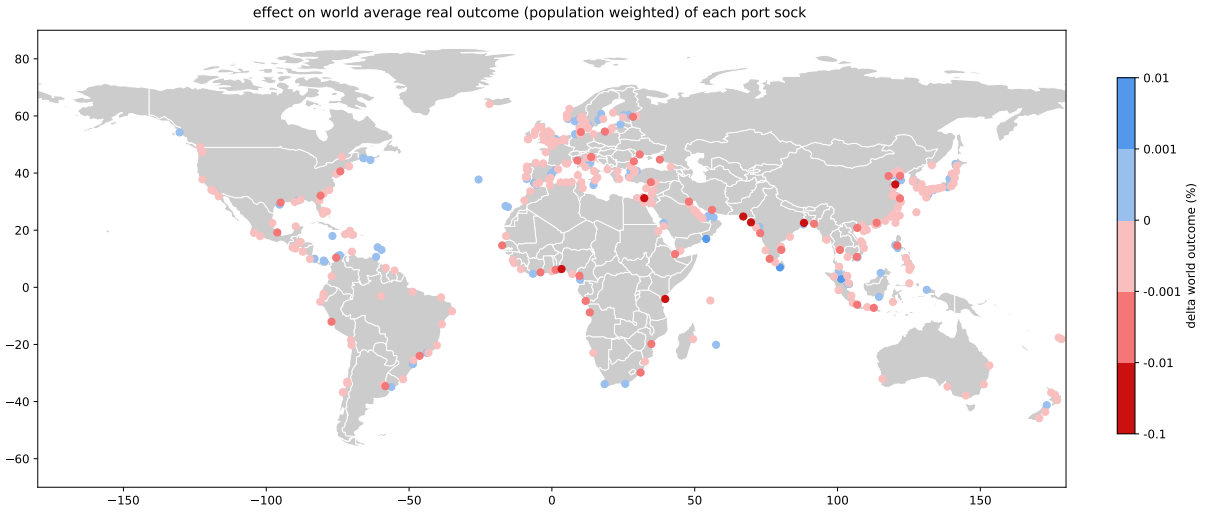
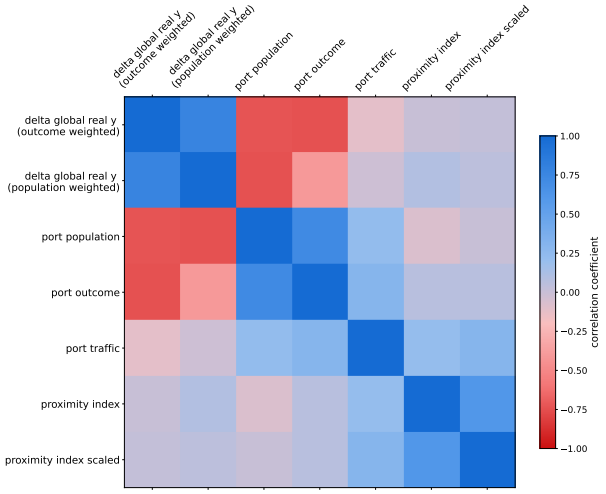


Figure 11: Correlation matrix of port caracteristics



6 Conclusion

I examine the economic impact of weather shocks affecting port infrastructures in the shipping network. I focus on the port congestion created by adverse weather conditions, that increases the cost of port services for ships. The framework provided allows to understand the spillovers mechanisms created by the network structure of shipping: the port inter-linkages spread the effect of local weather shocks, generating potential ripple effects – but also substitution mechanisms. A policy implication of this work is about infrastructures decisions to protect ports against adverse weather (Christodoulou et al., 2019): some ports are particularly critical for global welfare, and several countries would benefit from their protection. Computing counterfactuals based on

projections of sea weather is work in progress. This will allow to quantify the global effect of climate change on ports, as well as the distribution of potentially heterogeneous local effects.

References

Allen, T. & Arkolakis, C. (2014). Trade and the topography of the spatial economy. *The Quarterly Journal of Economics*, 129(3), 1085–1140.

Allen, T. & Arkolakis, C. (2022). The welfare effects of transportation infrastructure improvements. *The Review of Economic Studies*, 89(6), 2911–2957.

Anderson, J. E. & Van Wincoop, E. (2003). Gravity with gravitas: A solution to the border puzzle. *American economic review*, 93(1), 170–192.

Arkolakis, C., Costinot, A., & Rodríguez-Clare, A. (2012). New trade models, same old gains? *American Economic Review*, 102(1), 94–130.

Balboni, C., Boehm, J., & Waseem, M. (2023). Firm adaptation and production networks: Structural evidence from extreme weather events in pakistan.

Becker, A., Ng, A. K., McEvoy, D., & Mullett, J. (2018). Implications of climate change for shipping: Ports and supply chains. *Wiley Interdisciplinary Reviews: Climate Change*, 9(2), e508.

Brancaccio, G., Kalouptsidi, M., & Papageorgiou, T. (2020). Geography, transportation, and endogenous trade costs. *Econometrica*, 88(2), 657–691.

Brancaccio, G., Kalouptsidi, M., & Papageorgiou, T. (2024). Investment in infrastructure and trade: The case of ports. *National Bureau of Economic Research Working Paper*.

Carleton, T., Jina, A., Delgado, M., Greenstone, M., Houser, T., Hsiang, S., Hultgren, A., Kopp, R. E., McCusker, K. E., Nath, I., et al. (2022). Valuing the global mortality consequences of climate change accounting for adaptation costs and benefits. *The Quarterly Journal of Economics*, 137(4), 2037–2105.

Christodoulou, A., Christidis, P., & Demirel, H. (2019). Sea-level rise in ports: a wider focus on impacts. *Maritime Economics & Logistics*, 21, 482–496.

CIESIN (2018). Gridded population of the world, version 4.11 (gpwv4): Population count. Revision 11. Palisades, NY: NASA Socioeconomic Data and Applications Center (SEDAC).

Costinot, A. & Rodríguez-Clare, A. (2014). Trade theory with numbers: Quantifying the consequences of globalization. In *Handbook of international economics*, volume 4 (pp. 197–261). Elsevier.

Dell, M., Jones, B. F., & Olken, B. A. (2012). Temperature shocks and economic growth: Evidence from the last half century. *American Economic Journal: Macroeconomics*, 4(3), 66–95.

Deryugina, T., Kawano, L., & Levitt, S. (2018). The economic impact of hurricane katrina on its victims: Evidence from individual tax returns. *American Economic Journal: Applied Economics*, 10(2), 202–233.

Donaldson, D. & Hornbeck, R. (2016). Railroads and american economic growth: A "market access" approach. *The Quarterly Journal of Economics*, 131(2), 799–858.

Dube, A., Girardi, D., Jorda, O., & Taylor, A. M. (2023). *A local projections approach to difference-in-differences event studies*. Technical report, National Bureau of Economic Research.

Eaton, J. & Kortum, S. (2002). Technology, geography, and trade. *Econometrica*, 70(5), 1741–1779.

Fajgelbaum, P. D. & Schaal, E. (2020). Optimal transport networks in spatial equilibrium. *Econometrica*, 88(4), 1411–1452.

Fontagné, L., Lebrand, M. S. M., Murray, S., Santoni, G., & Ruta, M. (2023). Trade and infrastructure integration in africa. *Available at SSRN 4672520*.

Fuchs, S. & Wong, W. F. (2024). Multimodal transport networks. *Mimeo*.

Ganapati, S., Wong, W. F., & Ziv, O. (2021). Entrepot: Hubs, scale, and trade costs. *National Bureau of Economic Research Working Paper*.

Heiland, I., Moxnes, A., Ulltveit-Moe, K. H., & Zi, Y. (2019). Trade from space: Shipping networks and the global implications of local shocks. *CEPR Discussion Paper No. DP14193*.

Hersbach, H., Bell, B., Berrisford, P., Biavati, G., Horányi, A., Sabater, J. M., Nicolas, J., Peubey, C., Radu, R., Rozum, I., et al. (2023). Era5 hourly data on pressure levels from 1940 to present: Tech. rep.

Hummels, D. L. & Schaur, G. (2013). Time as a trade barrier. *American Economic Review*, 103(7), 2935–2959.

Izaguirre, C., Losada, I. J., Camus, P., Vigh, J. L., & Stenek, V. (2021). Climate change risk to global port operations. *Nature Climate Change*, 11(1), 14–20.

Ludwig, P. (2024). Can unilateral policy decarbonize maritime trade?

Mayer, T., Santoni, G., & Vicard, V. (2023). *The CEPII trade and production database*. CEPII.

OpenRouteService (2025). Openrouteservice api documentation. https://openrouteservice.org. Heidelberg Institute for Geoinformation Technology. Accessed: 2025-02-26.

Ossa, R. (2016). Quantitative models of commercial policy. In *Handbook of commercial policy*, volume 1 (pp. 207–259). Elsevier.

Pörtner, H.-O., Roberts, D. C., Masson-Delmotte, V., Zhai, P., Tignor, M., Poloczanska, E., Weyer, N., et al. (2019). The ocean and cryosphere in a changing climate. *IPCC special report on the ocean and cryosphere in a changing climate*, 1155, 10–1017.

UNCTAD (2023). *Review of Maritime Transport*. Technical report.

Wang, D., Guan, D., Zhu, S., Kinnon, M. M., Geng, G., Zhang, Q., Zheng, H., Lei, T., Shao, S., Gong, P., et al. (2021). Economic footprint of california wildfires in 2018. *Nature Sustainability*, 4(3), 252–260.

Appendix

A Model derivations

A.1 Equilibrium equations

Combining equations 10 and 13 yields (using additionally that $Y_i = w_i L_i$):

$$\Pi_i = \bar{A}_i l_i y_i^{-\frac{\theta+1}{\theta}} \bar{L}^{1-\frac{\theta+1}{\theta}} \tag{A.1}$$

The market clearing condition $Y_i = \sum_j X_{ij}$ from 12 can be rewritten using 13 as

$$\Pi_i^{-\theta} = \sum_j \tau_{ij}^{-\theta} E_j P_j^{\theta} \tag{A.2}$$

With the unbalanced trade assumption 15, I can write the first equilibrium equation:

$$\bar{A}_i^{-\theta} \bar{l}_i^{-\theta} y_i^{1+\theta} = \sum_j \tau_{ij}^{-\theta} (1+\kappa_j) y_j P_j^{\theta} \tag{A.3}$$

Similarly, combining the market clearing condition $E_i = \sum_j X_{ji}$ from 12 with 13 yields

$$P_i^{-\theta} = \sum_j \tau_{ji}^{-\theta} Y_j \Pi_j^{\theta} \tag{A.4}$$

Here no need to account for deficit, it directly leads to the second equilibrium equation:

$$P_i^{-\theta} = \sum_j \tau_{ji}^{-\theta} \bar{A}_j^{\theta} \bar{l}_j^{\theta} y_j^{-(\theta+1)} \tag{A.5}$$

A.2 Transportation costs

Starting from $\tau_{ij}^{-\theta} = \sum_{r \in \mathcal{R}_{ij}} \left(\prod_{l=0}^{K} p_{r_l}^{-\theta} \right) \left(\prod_{l=1}^{K} t_{r_{l-1},r_l}^{-\theta} \right)$ (coming from equation 11), I follow A&A into enumerating all the possible routes going from i to j of length K :

$$\tau_{ij}^{-\theta} = \sum_{K=0}^{+\infty} \left(\sum_{k_1=1}^{N} \sum_{k_2=1}^{N} \dots \sum_{k_{K-1}=1}^{N} p_i^{-\theta} t_{i,k_1}^{-\theta} p_{k_1}^{-\theta} t_{k_1,k_2}^{-\theta} \dots p_{k_{K-1}}^{-\theta} t_{k_{K-1},j}^{-\theta} p_j^{-\theta} \right) \tag{A.6}$$

I then adapt the matrix algebra of A&A to simplify this expression. In equation A.6, one can group an origin port with the link after, i.e. consider $g_{ij} \equiv p_i^{-\theta} t_{ij}^{-\theta}$. In which case,

$$\tau_{ij}^{-\theta} = \sum_{K=0}^{+\infty} (\mathbf{G}^K)_{ij} \, p_j^{-\theta} \quad \text{then} \quad \sum_{K=0}^{+\infty} \mathbf{G}^K = (\mathbf{I} - \mathbf{G})^{-1} \equiv \mathbf{C}^G \quad \Rightarrow \quad \tau_{ij}^{-\theta} = c_{ij}^G \, p_j^{-\theta} \tag{A.7}$$

Another alternative to simplify equation A.6 is to group an origin port with the link before, i.e. consider $d_{ij} \equiv t_{ij}^{-\theta} p_j^{-\theta}$. Then,

$$\tau_{ij}^{-\theta} = \sum_{K=0}^{+\infty} (\mathbf{D}^K)_{ij}\, p_i^{-\theta} \quad \text{then} \quad \sum_{K=0}^{+\infty} \mathbf{D}^K = (\mathbf{I} - \mathbf{D})^{-1} \equiv \mathbf{C}^D \quad \Rightarrow \quad \tau_{ij}^{-\theta} = c_{ij}^D\, p_i^{-\theta} \tag{A.8}$$

Equations A.7 and A.8 provide two alternative analytical relationships between transportation network and transportation costs.

A.3 Traffic Gravity equations

Let π_{ij}^k denote the expected number of times in which a node k is used in trade between i and j, π_{ij}^k:

$$\pi_{ij}^k = \sum_{r \in \mathcal{R}_{ij}} \left(\frac{\pi_{ij,r}}{\sum_{r' \in \mathcal{R}_{ij}} \pi_{ij,r'}} \right) n_r^k \tag{A.9}$$

where n_r^k is the number of times the route r passes through node k. Combining with equation 9 yields:

$$\pi_{ij}^k = \tau_{ij}^{\theta} \left(\sum_{r \in \mathcal{R}_{ij}} \left(\prod_{l=0}^{K} p_{r_l}^{-\theta} \right) \left(\prod_{l=1}^{K} t_{r_{l-1},r_l}^{-\theta} \right) \right) n_r^k$$

I then enumerating explicitly all possible routes going from i to j through k. Routes can have different lengths K (equal to the number of links, or the number of ports -1). A route of length K can go through node k at position $B \in \{0, 1, ..., K\}$. Isolating the cost on the left of k and the cost on the right of k leads to:

$$\pi_{ij}^k = \tau_{ij}^{\theta} \sum_{K=0}^{\infty} \sum_{B=0}^{K-1} \left(\sum_{r \in \mathcal{R}_{ik,B}} \prod_{n=1}^{B} g_{r_{n-1},r_n} \right) p_k^{-\theta} \left(\sum_{r \in \mathcal{R}_{kj,K-B}} \prod_{n=1}^{K-B} d_{r_{n-1},r_n} \right)$$

Using the same computation tricks as above:

$$\pi_{ij}^k = \tau_{ij}^{\theta} \sum_{K=0}^{\infty} \sum_{B=0}^{K-1} (\mathbf{G}^B)_{ij}\, p_k^{-\theta}\, (\mathbf{D}^{K-B})_{ij} \tag{A.10}$$

With some matrix algebra, one can show that

$$\sum_{K=0}^{+\infty} \sum_{B=0}^{K-1} \mathbf{G}^B\, \mathbf{P}\, \mathbf{D}^{K-B} = (\mathbf{I} - \mathbf{G})^{-1}\, \mathbf{P}\, (\mathbf{I} - \mathbf{D})^{-1}$$

Using the notations from the equations A.7 and A.8:

$$\pi_{ij}^{k} = \frac{c_{ik}^{G}\, p_k^{-\theta}\, c_{kj}^{D}}{\tau_{ij}^{\theta}} = \frac{\tau_{ik}^{-\theta}\, p_k^{\theta}\, \tau_{kj}^{-\theta}}{\tau_{ij}^{\theta}} \tag{A.11}$$

Let Ξ_k be the node traffic in location k, i.e. the value of all goods going through node k (either because they have k as an origin or destination, or just because they transit through k as an intermediate node along their route):

$$\Xi_k = \sum_{i \in \mathcal{N}} \sum_{j \in \mathcal{N}} \pi_{ij}^{k} X_{ij} \tag{A.12}$$

Substituting for X_{ij} with equation 13, I find that equation A.12 can be written as gravity equation for node traffic, with the same market access terms as a the gravity equation for trade flows 13:

$$\Xi_k = p_k^{\theta} \times P_k^{-\theta} \times \Pi_k^{-\theta} \tag{A.13}$$

A&A also show that similarly, link traffic Ξ_{kl} can be expressed with a gravity equation for link traffic:

$$\pi_{ij}^{kl} = \frac{\tau_{ik}^{-\theta}\, t_{kl}^{-\theta}\, \tau_{lj}^{-\theta}}{\tau_{ij}^{\theta}} \tag{A.14}$$

$$\Xi_{kl} = t_{lk}^{-\theta} \times P_k^{-\theta} \times \Pi_l^{-\theta} \tag{A.15}$$

A.4 Traffic and trade

Writing equation 13 in matrix notations – where $[x_{ij}]$ denotes a $N \times N$ matrix of general term x_{ij}, and $\text{diag}\,(x_i)$ a $N \times N$ diagonal matrix where the diagonal term of the i-th row is equal to x_i:

$$[X_{ij}] = \text{diag}\left(\frac{Y_i}{\Pi_i^{-\theta}}\right) \left[\tau_{ij}^{-\theta}\right] \text{diag}\left(\frac{E_i}{P_i^{-\theta}}\right) \tag{A.16}$$

Combining with equation A.8, it yields

$$[X_{ij}] = \text{diag}\left(\frac{Y_i}{\Pi_i^{-\theta}} p_i^{-\theta}\right) (\mathbf{I} - \mathbf{D})^{-1} \text{diag}\left(\frac{E_i}{P_i^{-\theta}}\right) \tag{A.17}$$

with

$$\mathbf{D} = [d_{ij}] = \left[\tau_{ij}^{-\theta}\right] \text{diag}\left(p_i^{-\theta}\right)$$

It comes

$$[X_{ij}] = \text{diag}\left(\frac{Y_i}{\Pi_i^{-\theta}} p_i^{-\theta}\right) \left(\mathbf{I} - \left[\tau_{ij}^{-\theta}\right] \text{diag}\left(p_i^{-\theta}\right)\right)^{-1} \text{diag}\left(\frac{E_i}{P_i^{-\theta}}\right) \tag{A.18}$$

Similarly, writing equation 24 in matrix notations:

$$[\Xi_{ij}] = \text{diag}\left(P_i^{-\theta}\right)\left[t_{ij}^{-\theta}\right]\text{diag}\left(\Pi_i^{-\theta}\right) \tag{A.19}$$

Inverting, it comes:

$$\left[t_{ij}^{-\theta}\right] = \text{diag}\left(P_i^{\theta}\right)[\Xi_{ij}]\,\text{diag}\left(\Pi_i^{\theta}\right) \tag{A.20}$$

Combining equations A.18 and A.20:

$$[X_{ij}] = \text{diag}\left(\frac{Y_i}{\Pi_i^{-\theta}}p_i^{-\theta}\right)\left(\mathbf{I} - \text{diag}\left(P_i^{\theta}\right)[\Xi_{ij}]\,\text{diag}\left(\Pi_i^{\theta}\right)\text{diag}\left(p_i^{-\theta}\right)\right)^{-1}\text{diag}\left(\frac{E_i}{P_i^{-\theta}}\right) \tag{A.21}$$

Inverting the matrices:

$$[X_{ij}]^{-1} = \text{diag}\left(E_i^{-1}\right)\left(\text{diag}\left(P_i^{-\theta}\right)\text{diag}\left(\Pi_i^{-\theta}\right)\text{diag}\left(p_i^{\theta}\right) - [\Xi_{ij}]\right)\text{diag}\left(Y_i^{-1}\right) \tag{A.22}$$

And inverting again:

$$[X_{ij}] = \text{diag}\left(Y_i\right)\left(\text{diag}\left(P_i^{-\theta}\right)\text{diag}\left(\Pi_i^{-\theta}\right)\text{diag}\left(p_i^{\theta}\right) - [\Xi_{ij}]\right)^{-1}\text{diag}\left(E_i\right) \tag{A.23}$$

The objective is now to express $\text{diag}\left(\Pi_i^{-\theta}\right)\text{diag}\left(p_i^{\theta}\right)$ as a function of observables only.

Starting from the definition $P_i^{-\theta} = \sum_j \tau_{ji}^{-\theta}\frac{Y_j}{\Pi_j^{-\theta}}$ and switching to matrix notations – where where $[x_i]$ denotes a $N \times 1$ column matrix of general term x_i:

$$\left[P_i^{-\theta}\right] = \left[\tau_{ij}^{-\theta}\right]'\left[\frac{Y_i}{\Pi_i^{-\theta}}\right] \tag{A.24}$$

$$\left[P_i^{-\theta}\right] = \left(\mathbf{I} - \mathbf{D}'\right)^{-1}\left[p_i^{-\theta}\frac{Y_i}{\Pi_i^{-\theta}}\right] \tag{A.25}$$

$$\left(\mathbf{I} - \text{diag}\left(p_i^{-\theta}\right)\text{diag}\left(\Pi_i^{\theta}\right)[\Xi_{ij}]'\,\text{diag}\left(P_i^{\theta}\right)\right)\left[P_i^{-\theta}\right] = \left[p_i^{-\theta}\frac{Y_i}{\Pi_i^{-\theta}}\right] \tag{A.26}$$

$$\left[\Pi_i^{-\theta}P_i^{-\theta}p_i^{\theta}\right] = [Y_i] + [\Xi_{ij}]'\,[1] \tag{A.27}$$

where $[1]$ is a $N \times 1$ column matrix in which all coefficients are equal to 1.

Similarly, starting from the definition $\Pi_i^{-\theta} = \sum_j \tau_{ij}^{-\theta}\frac{E_j}{P_j^{-\theta}}$ and switching to matrix notations:

$$\left[\Pi_i^{-\theta}\right] = \left[\tau_{ij}^{-\theta}\right]\left[\frac{E_i}{P_i^{-\theta}}\right] \tag{A.28}$$

$$\left[\Pi_i^{-\theta}\right] = (\mathbf{I} - \mathbf{G})^{-1} \left[p_i^{-\theta} \frac{E_i}{P_i^{-\theta}}\right] \tag{A.29}$$

with

$$\mathbf{G} = [g_{ij}] = \text{diag}\left(p_i^{-\theta}\right) \left[\tau_{ij}^{-\theta}\right]$$

$$\left(\mathbf{I} - \text{diag}\left(p_i^{-\theta}\right) \text{diag}\left(P_i^{\theta}\right) [\Xi_{ij}] \, \text{diag}\left(\Pi_i^{\theta}\right)\right) \left[\Pi_i^{-\theta}\right] = \left[p_i^{-\theta} \frac{E_i}{P_i^{-\theta}}\right] \tag{A.30}$$

$$\left[\Pi_i^{-\theta} P_i^{-\theta} p_i^{\theta}\right] = [E_i] + [\Xi_{ij}] \, [1] \tag{A.31}$$

where $[1]$ is a $N \times 1$ column matrix in which all coefficients are equal to 1.

Following A&A, I average the two definitions of $\text{diag}\left(\Pi_i^{-\theta}\right) \text{diag}\left(p_i^{\theta}\right)$:

$$\left[\Pi_i^{-\theta} P_i^{-\theta} p_i^{\theta}\right] = \frac{1}{2} [Y_i + E_i] + \frac{1}{2} \left([\Xi_{ij}]' \, [1] + [\Xi_{ij}] \, [1]\right) \tag{A.32}$$

Finally, plugging into the expression of $[X_{ij}]$ in equation A.23:

$$[X_{ij}] = \text{diag}\,(Y_i) \left(\text{diag}\left(\frac{1}{2} [Y_i + E_i] + \frac{1}{2} \left([\Xi_{ij}]' \, [1] + [\Xi_{ij}] \, [1]\right)\right) - [\Xi_{ij}]\right)^{-1} \text{diag}\,(E_i) \tag{A.33}$$

i.e., back to vectors notations:

$$X_{ij} = Y_i \left(\mathbf{D}^{\mathbf{X}} - [\Xi_{ij}]\right)^{-1}_{ij} E_j \tag{A.34}$$

where $\mathbf{D}^{\mathbf{X}} = \text{diag}\left(\frac{1}{2} [Y_i + E_i] + \frac{1}{2} \left([\Xi_{ij}]' \, [1] + [\Xi_{ij}] \, [1]\right)\right)$

A.5 Equilibrium with traffic

The first step consists in integrating the analytical relationship between τ_{ij} and t_{ij}, p_i into the equilibrium equations 16 and 17. Starting from the first equilibrium equation 16 and using expression A.7 yields:

$$\bar{A}_i^{-\theta} \bar{l}_i^{-\theta} y_i^{1+\theta} = \sum_j c_{ij}^G p_j^{-\theta} (1 + \kappa_j) y_j P_j^{\theta} \tag{A.35}$$

Switching to matrix notations:

$$\left[\bar{A}_i^{-\theta} \bar{l}_i^{-\theta} y_i^{1+\theta}\right] = \mathbf{C}^{\mathbf{G}} \left[p_i^{-\theta} (1 + \kappa_i) y_i P_i^{\theta}\right] \tag{A.36}$$

where $\left[\bar{A}_i^{-\theta} \bar{l}_i^{-\theta} y_i^{1+\theta}\right]$ and $\left[p_i^{-\theta} (1 + \kappa_i) y_i P_i^{\theta}\right]$ are $N \times 1$ column matrices and $\mathbf{C}^{\mathbf{G}}$ is a $N \times N$

square matrix. Remember that $\mathbf{C^G} = (\mathbf{I} - \mathbf{G})^{-1}$ from A.7, which yields:

$$(\mathbf{I} - \mathbf{G}) \left[\bar{A}_i^{-\theta} \bar{l}_i^{-\theta} y_i^{1+\theta} \right] = \left[p_i^{-\theta} (1 + \kappa_i) y_i P_i^{\theta} \right] \tag{A.37}$$

or in non-matrix notations:

$$\bar{A}_i^{-\theta} \bar{l}_i^{-\theta} y_i^{1+\theta} = p_i^{-\theta} (1 + \kappa_i) y_i P_i^{\theta} + \sum_j p_i^{-\theta} t_{ij}^{-\theta} \bar{A}_j \bar{l}_j^{-\theta} y_j^{\theta+1} \tag{A.38}$$

Similarly with the second equilibrium equation 17 and using expression A.8:

$$P_i^{-\theta} = \sum_j c_{ji}^{D} p_j^{-\theta} \bar{A}_j^{\theta} \bar{l}_j^{\theta} y_j^{-(\theta+1)} \tag{A.39}$$

Switching to matrix notations:

$$\left[P_i^{-\theta} \right] = \left[p_i^{-\theta} \bar{A}_i^{\theta} \bar{l}_i^{\theta} y_i^{-(\theta+1)} \right] \mathbf{C^{D'}} \tag{A.40}$$

where $\left[P_i^{-\theta} \right]$ and $\left[p_i^{-\theta} \bar{A}_i^{\theta} \bar{l}_i^{\theta} y_i^{-(\theta+1)} \right]$ are $N \times 1$ column matrices and $\mathbf{C^D}$ is a $N \times N$ square matrix. Remember that $\mathbf{C^D} = (\mathbf{I} - \mathbf{D})^{-1}$ from A.7, hence $\mathbf{C^{D'}} = (\mathbf{I} - \mathbf{D'})^{-1}$, which yields:

$$\left[P_i^{-\theta} \right] (\mathbf{I} - \mathbf{D'}) = \left[p_i^{-\theta} \bar{A}_i^{\theta} \bar{l}_i^{\theta} y_i^{-(\theta+1)} \right] \tag{A.41}$$

or in non-matrix notations:

$$P_i^{-\theta} = p_i^{-\theta} \bar{A}_i^{\theta} \bar{l}_i^{\theta} y_i^{-(\theta+1)} + \sum_j p_i^{-\theta} t_{ji}^{-\theta} P_j^{-\theta} \tag{A.42}$$

The second step consists in introducing the traffic congestion into equations A.38 and A.42. Combining equation 30 with expression A.1 yields

$$p_i = \bar{\Gamma}_i^{\frac{1}{1-\lambda\theta}} \, e^{\frac{\mu}{1-\lambda\theta} \, \text{weather}_i} \, \bar{L}^{\frac{\lambda}{1-\lambda\theta}} \bar{A}_i^{\frac{-\lambda\theta}{1-\lambda\theta}} \bar{l}_i^{\frac{-\lambda\theta}{1-\lambda\theta}} P_i^{\frac{-\lambda\theta}{1-\lambda\theta}} \, y_i^{\frac{\lambda(\theta+1)}{1-\lambda\theta}} \tag{A.43}$$

Using this expression to replace p_i in equations A.38 and A.42 leads to the two equilibrium conditions with traffic:

$$\begin{aligned} y_i^{\theta+1+\frac{\lambda\theta(\theta+1)}{1-\lambda\theta}} P_i^{-\frac{\lambda\theta^2}{1-\lambda\theta}} =& \bar{L}^{-\frac{\lambda\theta}{1-\lambda\theta}} \bar{A}_i^{\frac{\lambda\theta^2}{1-\lambda\theta}+\theta} \bar{\Gamma}_i^{\frac{-\theta}{1-\lambda\theta}} e^{\frac{-\mu\theta}{1-\lambda\theta}\text{weather}_i} \bar{l}_i^{\frac{\lambda\theta^2}{1-\lambda\theta}+\theta} (1 + \kappa_i) y_i P_i^{\theta} \\ &+ \bar{L}^{-\frac{\lambda\theta}{1-\lambda\theta}} \sum_{j=1}^{N} \bar{A}_i^{\frac{\lambda\theta^2}{1-\lambda\theta}+\theta} \bar{A}_j \bar{t}_{ij}^{-\theta} \bar{\Gamma}_i^{\frac{-\theta}{1-\lambda\theta}} e^{\frac{-\mu\theta}{1-\lambda\theta}\text{weather}_i} \bar{l}_i^{\frac{\lambda\theta^2}{1-\lambda\theta}+\theta} \bar{l}_j^{-\theta} y_j^{1+\theta} \end{aligned} \tag{A.44}$$

$$
\begin{aligned}
y_i^{\frac{\lambda\theta(\theta+1)}{1-\lambda\theta}} P_i^{-\theta-\frac{\lambda\theta^2}{1-\lambda\theta}} =& \bar{L}^{\frac{-\lambda\theta}{1-\lambda\theta}} \bar{A}_i^{\frac{\lambda\theta^2}{1-\lambda\theta}+\theta} \bar{\Gamma}_i^{\frac{-\theta}{1-\lambda\theta}} e^{\frac{-\mu\theta}{1-\lambda\theta}\text{weather}_i} \bar{l}_i^{\frac{\lambda\theta^2}{1-\lambda\theta}+\theta} y_i^{-\theta+1} \\
&+ \bar{L}^{-\frac{\lambda\theta}{1-\lambda\theta}} \sum_{j=1}^{N} \bar{A}_i^{\frac{\lambda\theta^2}{1-\lambda\theta}} \bar{t}_{ij}^{-\theta} \bar{\Gamma}_i^{\frac{-\theta}{1-\lambda\theta}} e^{\frac{-\mu\theta}{1-\lambda\theta}\text{weather}_i} \bar{l}_i^{\frac{\lambda\theta^2}{1-\lambda\theta}} P_j^{-\theta}
\end{aligned} \tag{A.45}
$$

A.6 Exact hat algebra

Consider a counterfactual weather $\{\text{weather}'_i\}_{i\in\mathcal{N}}$ and counterfactual trade deficits $\{(1+\kappa'_i)\}_{i\in\mathcal{N}}$. Combining the market clearing condition $Y_i = \sum_j X_{ij}$ from 12 with equation 13 yields

$$
\Pi_i^{-\theta} = \sum_j \tau_{ij}^{-\theta} E_j P_j^{\theta} \tag{A.46}
$$

Using equation A.8 and switching to matrix notations, it comes:

$$
\left[\Pi_i^{-\theta}\right] = \left(\mathbf{I} - \left[p_i^{-\theta} t_{ij}^{-\theta}\right]\right)^{-1} \left[p_i^{-\theta} E_i P_i^{\theta}\right] \tag{A.47}
$$

where $\left[\Pi_i^{-\theta}\right]$ and $\left[p_i^{-\theta} E_i P_i^{\theta}\right]$ are $N \times 1$ column matrices and $\left[p_i^{-\theta} t_{ij}^{-\theta}\right]$ is a $N \times N$ square matrix. This can be rewritten as

$$
\Pi_i^{-\theta} = p_i^{-\theta} E_i P_i^{\theta} + \sum_j p_i^{-\theta} t_{ij}^{-\theta} \Pi_j^{-\theta} \tag{A.48}
$$

Similarly, combining the market clearing condition $E_j = \sum_i X_{ij}$ from 12 with equation 13 yields

$$
P_j^{-\theta} = \sum_j \tau_{ij}^{-\theta} Y_i \Pi_i^{\theta} \tag{A.49}
$$

Using equation A.7 and switching to matrix notations, it comes:

$$
\left[P_i^{-\theta}\right]' = \left[p_i^{-\theta} Y_i \Pi_i^{\theta}\right]' \left(\mathbf{I} - \left[p_j^{-\theta} t_{ij}^{-\theta}\right]\right)^{-1} \tag{A.50}
$$

which can be rewritten as

$$
P_j^{-\theta} = p_j^{-\theta} Y_j \Pi_j^{\theta} + \sum_i p_j^{-\theta} t_{ij}^{-\theta} P_i^{-\theta} \tag{A.51}
$$

In the counterfactual scenario, equation A.48 will be:

$$
\Pi_i'^{-\theta} = p_i'^{-\theta} E_i' P_i'^{\theta} + \sum_j p_i'^{-\theta} \bar{t}_{ij}^{-\theta} \Pi_j'^{-\theta} \tag{A.52}
$$

where x' denote the counterfactual value of variable x. $\bar{t}_{ij}$ stays the same in the counterfactual world as it is exogenously given, hence not affected by a change in weather. Using the notation $\hat{x}_i \equiv \frac{x'_i}{x_i}$:

$$
\hat{\Pi}_i'^{-\theta} = \frac{1}{\Pi_i^{-\theta}} p_i^{-\theta} E_i P_i^{\theta} \hat{p}_i^{-\theta} \hat{E}_i \hat{P}_i^{\theta} + \sum_j \frac{1}{\Pi_i^{-\theta}} p_i^{-\theta} \bar{t}_{ij}^{-\theta} \Pi_j^{-\theta} \hat{p}_i^{-\theta} \hat{\Pi}_j^{-\theta} \tag{A.53}
$$

Using A.48 to replace $\Pi_i^{-\theta}$ and simplifying yields:

$$\hat{\Pi}_i'^{-\theta} = \frac{E_i}{E_i + \sum_j \bar{t}_{ij} P_i^{-\theta} \Pi_j^{-\theta}} \hat{p}_i^{-\theta} \hat{E}_i \hat{P}_i^{\theta} + \sum_j \left(\frac{\bar{t}_{ij} P_i^{-\theta} \Pi_j^{-\theta}}{E_i + \sum_j \bar{t}_{ij} P_i^{-\theta} \Pi_j^{-\theta}} \right) \hat{p}_i^{-\theta} \hat{\Pi}_j^{-\theta} \tag{A.54}$$

Remember that $\Xi_{ij} = \bar{t}_{ij} P_i^{-\theta} \Pi_j^{-\theta}$ (equation 24). Hence:

$$\hat{\Pi}_i^{-\theta} = \frac{E_i}{E_i + \sum_j \Xi_{ij}} \hat{p}_i^{-\theta} \hat{E}_i \hat{P}_i^{\theta} + \sum_j \left(\frac{\Xi_{ij}}{E_i + \sum_j \Xi_{ij}} \right) \hat{p}_i^{-\theta} \hat{\Pi}_j^{-\theta} \tag{A.55}$$

Similarly, equation A.51 will be in the counterfactual world:

$$P_j'^{-\theta} = p_j'^{-\theta} Y_j' \Pi_j'^{\theta} + \sum_i p_j'^{-\theta} \bar{t}_{ij}^{-\theta} P_i'^{-\theta} \tag{A.56}$$

which can be rewritten as:

$$\hat{P}_j^{-\theta} = \frac{1}{P_j^{-\theta}} \frac{p_j^{-\theta} Y_j}{\Pi_j^{-\theta}} \frac{\hat{p}_j^{-\theta} \hat{Y}_j}{\hat{\Pi}_j^{-\theta}} + \sum_i \frac{p_j^{-\theta} \bar{t}_{ij}^{-\theta} P_i^{-\theta}}{P_j^{-\theta}} \hat{p}_j^{-\theta} \hat{P}_i^{-\theta} \tag{A.57}$$

Using A.51 to replace $P_j^{-\theta}$ and the expression of Ξ_{ij} from equation 24 yields:

$$\hat{P}_j^{-\theta} = \frac{Y_j}{Y_j + \sum_i \Xi_{ij}} \frac{\hat{p}_j^{-\theta} \hat{Y}_j}{\hat{\Pi}_j^{-\theta}} + \sum_i \left(\frac{\Xi_{ij}}{Y_j + \sum_i \Xi_{ij}} \right) \hat{p}_j^{-\theta} \hat{P}_i^{-\theta} \tag{A.58}$$

From equation 30, we can write:

$$\hat{p}_i = e^{\frac{\mu}{1-\lambda\theta} \Delta \text{ weather}_i} \hat{P}_i^{\frac{-\lambda\theta}{1-\lambda\theta}} \hat{\Pi}_i^{\frac{-\lambda\theta}{1-\lambda\theta}} \tag{A.59}$$

Plugging this expression in equations A.55 and A.58 leads to:

$$\hat{\Pi}_i^{-\frac{\theta}{1-\lambda\theta}} \hat{P}_i^{-\frac{\theta}{1-\lambda\theta}} = \frac{E_i}{E_i + \sum_j \Xi_{ij}} \hat{E}_i \, e^{\frac{-\mu\theta}{1-\lambda\theta} \Delta \text{ weather}_i} + \sum_j \left(\frac{\Xi_{ij}}{E_i + \sum_j \Xi_{ij}} \right) e^{\frac{-\mu\theta}{1-\lambda\theta} \Delta \text{ weather}_i} \hat{P}_i^{-\theta} \hat{\Pi}_j^{-\theta} \tag{A.60}$$

$$\hat{P}_i^{-\frac{\theta}{1-\lambda\theta}} \hat{\Pi}_i^{-\frac{\theta}{1-\lambda\theta}} = \frac{Y_i}{Y_i + \sum_j \Xi_{ji}} \hat{Y}_i \, e^{\frac{-\mu\theta}{1-\lambda\theta} \Delta \text{ weather}_i} + \sum_j \left(\frac{\Xi_{ji}}{Y_i + \sum_j \Xi_{ji}} \right) e^{\frac{-\mu\theta}{1-\lambda\theta} \Delta \text{ weather}_i} \hat{P}_j^{-\theta} \hat{\Pi}_i^{-\theta} \tag{A.61}$$

Finally, from equation A.1 I get

$$\hat{\Pi}_i = \hat{y}_i^{-\frac{\theta+1}{\theta}} \tag{A.62}$$

and from equation 15 it comes

$$\hat{E}_i = \widehat{(1+\kappa_i)}\hat{y}_i \tag{A.63}$$

Plugging these two expressions into equations A.60 and A.61 yields the two exact hat equilibrium equations 33 and 34:

$$\begin{aligned}\hat{y}_i^{\frac{1+\theta}{1-\lambda\theta}}\hat{P}_i^{\frac{-\theta}{1-\lambda\theta}+\theta} = &\left(\frac{E_i}{E_i+\sum_j \Xi_{ij}}\right) e^{\frac{-\mu\theta}{1-\lambda\theta}\Delta\text{weather}_i}\widehat{(1+\kappa_i)}\hat{y}_i\hat{P}_i^{\theta} \\ &+\sum_{j=1}^{N}\left(\frac{\Xi_{ij}}{E_i+\sum_j \Xi_{ij}}\right) e^{\frac{-\mu\theta}{1-\lambda\theta}\Delta\text{weather}_i}\hat{y}_j^{\theta+1}\end{aligned} \tag{A.64}$$

$$\begin{aligned}\hat{y}_i^{\frac{\theta+1}{1-\lambda\theta}-(\theta+1)}\hat{P}_i^{\frac{-\theta}{1-\lambda\theta}} = &\left(\frac{Y_i}{Y_i+\sum_j \Xi_{ji}}\right) e^{\frac{-\mu\theta}{1-\lambda\theta}\Delta\text{weather}_i}\hat{y}_i^{-\theta} \\ &+\sum_{j=1}^{N}\left(\frac{\Xi_{ji}}{Y_i+\sum_j \Xi_{ji}}\right) e^{\frac{-\mu\theta}{1-\lambda\theta}\Delta\text{weather}_i}\hat{P}_j^{-\theta}\end{aligned} \tag{A.65}$$

B Data

Table B.1: Descriptive statistics of port efficiency measures built from AIS shipping data

	N	mean	sd	p25	median	p75
weekly number of calls	534,654	13.4	33.4	2	4	12
port-average weekly number of calls	1,665	10.1	28.3	1.4	2.8	7.7
weekly average dwell time (in hours)	534,654	42.4	158.1	12.8	24.2	43.7
port-average weekly average dwell time (in hours)	1,665	49.3	59.3	19.5	34.2	58.9

Note: Ports with more than 50 calls over the 2015-2023 period are included.

Table B.2: Descriptive statistics of port daily wave height

	N	mean	sd	p25	median	p75
daily wave height in ports (in meters)	5,223,201	0.86	0.66	0.37	0.69	1.17
port-average daily wave height (in meters)	1,679	0.85	0.47	0.51	0.74	1.10

Note: Ports with more than 50 calls over the 2015-2023 period are included.

C Further reduced-form evidence

C.1 Event-study setting

A weather shock might also have an effect before and after it is actually happening. To test this, I consider the effect of a binary treatment $\mathbb{1}\{\text{weather}_{it} > p99\text{weather}_i\}$ on the days before / after it happens, using an event study setting.[29] I rely on the local projection difference-in-differences (LP-DiD) setting of (Dube et al., 2023), to allow to non-absorbing treatment and potential multiple treatments:

$$y_{i,t+h} - y_{i,t-1} = \beta_h \Delta D_{it} + \delta_t^h + \delta_{im}^h + \epsilon_{it}^h \tag{C.66}$$

where D_{it} is the (binary) treatment status of port i on day t and Δ denotes first-difference operator, with sample restriction:

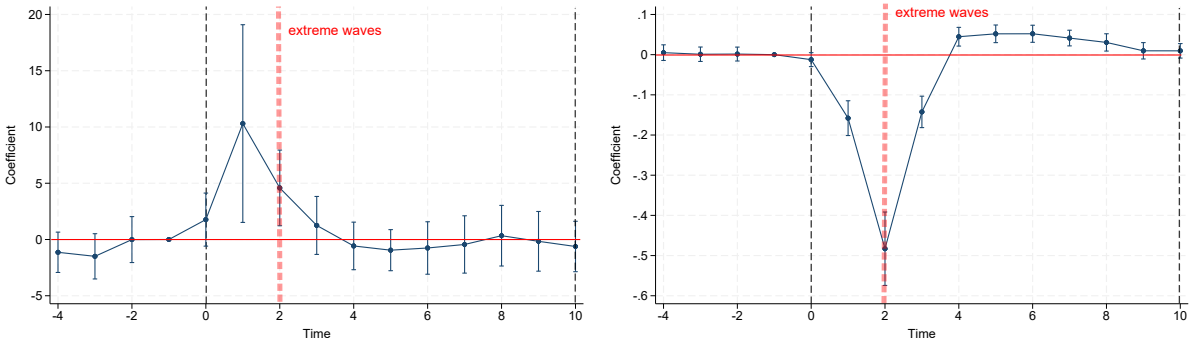
$$\begin{cases} \text{treatment:} & D_{i,t+j} = 1 \text{ for } 0 \leq j \leq h, \qquad D_{i,t-j} = 0 \text{ for } 1 \leq j \leq L \\ \text{clean control:} & D_{i,t-j} = 0 \text{ for } -h \leq j \leq L \end{cases} \tag{C.67}$$

where L is the number of periods after which the dynamic effects stabilize. I keep in the sample only clean treatment (ports that remain in treatment for the post-event window and that have not experienced a treatment close before the one we are considering) and clean controls (ports are not close to a treatment, either before or after). I also control for potential non-parallel trends with port-month fixed effects. To account for the fact that this setting assumes no anticipation and that the clean treated and control conditions assume no change of treatment status (i.e. no entry into treatment and no exit of treatment), I define treatment as 12 days around the extreme event (2 days before, 10 days after).

The results in Figure C.1 show that for dwell time, the effect is bigger one day before the event, but does not seem to last after. The number of port calls is reduced both before and after, but there seems to be a slight catch up afterwards – but which does not compensate the negative effect.

[29] With this definition of event, I am potentially comparing days where the wave height is above the 99th percentile, to days where it is slightly below: this would tend to attenuate the results.

Figure C.1: Event study results: effect extreme wave event on port efficiency



(a) Dwell time

(b) Number of entering calls

C.2 Reduced-form at the ship level

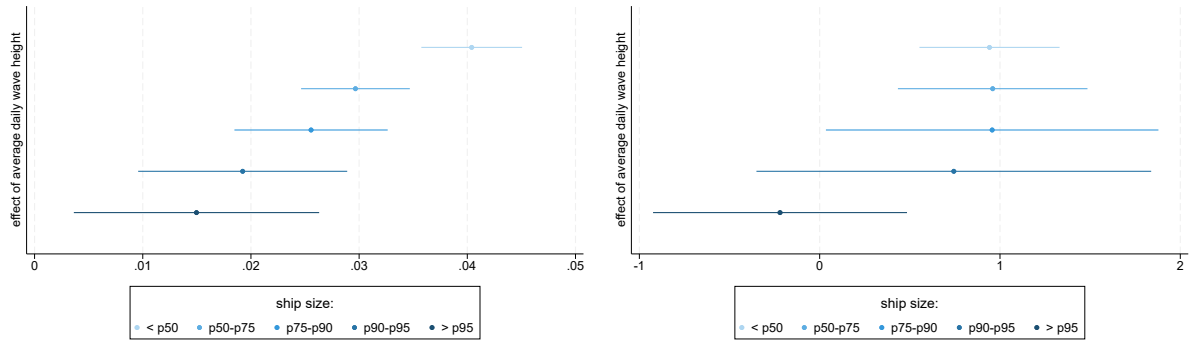
The data allow to estimate the effect of weather shocks on ships dwell time at the ship level (without aggregating to port daily averages):

$$\ln(\text{time}_{sit}) = \beta \text{ weather}_{it} + \delta_{si} + \delta_t + \delta_{iy} + \epsilon_{sit} \tag{C.68}$$

where s denotes a ship, i a port, t a day and y a year. time_{sit} is the dwell time experienced by ship s in port i on day t. weather_{it} is the weather at port i during day t – measured either by average daily wave height or by non-linear bins of wave height.

The results in Table C.3 show effects similar to what I find at the port level: a higher wave height increases ship dwell time, an effect which is mostly driven by extreme wave heights. An heterogeneity analysis by ship deadweight tonnage (Figure C.2) shows that the biggest ships are less likely to be impacted by wave height than the smallest ones.

Figure C.2: Heterogeneous effects of wave height by ship size



(a) on ship log dwell time

(b) on ship dwell time

Table C.3: Effect of wave height on ship dwell time

	(1)	(2)
average wave height	0.0347***	
	(0.0021)	
wave < p50		*ref*
wave p50-p90		0.0046***
		(0.0011)
wave p90-p99		0.0278***
		(0.0029)
wave > p50		0.0931***
		(0.0071)
date (day) FE	✓	✓
ship-port FE	✓	✓
port-year FE	✓	✓
SE cluster level	ship, port	ship, port
# observations	6,854,364	6,854,364
# ports	1,676	1,676

Standard errors in parentheses

* $p < 0.10$, ** $p < 0.05$, *** $p < 0.01$

C.3 Effects outside of the port

When a port is disrupted, ships might prefer to wait outside of the port, to avoid paying additional port fees. This mechanism is not captured in the baseline specification as port calls data only allow to observe when ships actually enter inside the port. However, I can look at the effect of weather shocks in origin or departure port, on the duration of ships trips – i.e. the amount of time between the moment they leave their origin port and the moment they arrive at their destination port. If ships tend to wait outside of ports when there is bad weather, this should increase their trip time.

I consider the following specification:

$$log(\text{trip time})_{sod,t} = \beta_o \text{ weather}_{o,t} + \beta_d \text{ weather}_{d,t+\text{trip time}} + \delta_s + \delta_{od} + \delta_t + \epsilon_{sod,t} \tag{C.69}$$

where $\text{trip time}_{sod,t}$ is the trip time of ship s going from origin port o to destination port d on day t (day of departure), $\text{weather}_{o,t}$ is the weather in port of origin at the day of departure, $\text{weather}_{d,t+\text{trip time}}$ the weather in port of destination at the day of arrival. I consider different sets of fixed effects: day, route, ship, ship-route, route-year.

Table C.4 shows the results, which seem constant over the different sets of fixed effects. They confirm the hypothesized mechanism: +1m in wave height at the origin port increases trip duration by 1.3%, while +1m in wave height at the destination port increases trip duration by 2.2%. In column (4), I remove the shortest routes (trimming at the top and bottom 25%) to make sure that the weather along the route is not correlated with weather in the ports of departure and arrival, and still find a positive and significant effect.

This means the effects measured *inside* the ports might be only a lower bound of the full effects, since they do not capture ships waiting *outside* of ports.

Table C.4: Effect of origin and destination ports wave height on ships trip duration

	(1)	(2)	(3)	(4)
wave height at origin port	0.0139***	0.0133***	0.0135***	0.0159***
	(0.0011)	(0.0012)	(0.0012)	(0.0015)
wave height at destination port	0.0222***	0.0224***	0.0224***	0.0279***
	(0.0011)	(0.0012)	(0.0012)	(0.0016)
date (day) FE	✓	✓	✓	✓
route (o-d) FE	✓			
ship FE	✓			
ship-route FE		✓	✓	✓
route-year FE			✓	✓
route distance restriction				✓
# observations	5,770,534	5,289,930	5,278,881	2,652,050
# routes	14,109	14,101	14,054	7,137

Standard errors in parentheses

* $p < 0.10$, ** $p < 0.05$, *** $p < 0.01$

C.4 Routes vs Ports

Delays in shipping can also happen because of weather conditions along the maritime route, i.e. in the journey between two ports. I compare the effects on shipping of weather along the maritime route and weather in the port, using the following specification:

$$\text{time}_{sit} = \beta \text{ weather}_{it} + \delta_{si} + \delta_t + \delta_{im} + \delta_{iy} + \epsilon_{sit} \tag{C.70}$$

where s is a ship, i either a *route* or a *port*, and t a day. time_{sit} denotes the time (in hours) spent by ship s along the route i or in the port i[30], $weather_{it}$ denotes the weather conditions (wave height) along the route i or in the port i – measured either as average daily wave height or bins of daily wave height. I also include ship-port (resp. ship-route) fixed effects, date fixed effects, port-month-of-the-year (resp. route-month-of-the-year) fixed effects, and port-year (resp. route-year) fixed effects.

To measure shipping time and weather along the maritime routes, I focus on trips happening on the 300 most frequent routes present in the shipping data. I compute trip duration as the difference between the time of destination port arrival and origin port departure. Since I only observe the origin and destination ports and not the exact trajectory of the ship in between, I rely on SeaRoute algorithm to compute the shortest route by sea between these two ports. Using gridded wave height from ERA5, I compute the weather along a route for a given day

[30]To ensure a better comparability between ports and routes, the dependent variable is in levels rather than in log, to quantify the effect in terms of additional hours of shipping.

as a weighted average of the grid points weather, where the weights are the inverse of distance between the grid point and the route, times a measure of the density of grid cells at the point location.

The results in Table C.5 show that the effect on weather along the route or in the port tend to be pretty similar: an increase of 1m of average wave height along the route or at the port increases shipping time by 0.7 hour. Port extreme weather events seems to have a slightly more important effect than route extreme weather events: a wave height greater than 2m at the port adds 1.5 hour of shipping time compared to a wave height lower than 0.5m, again 1.2 additional hour for a wave height greater than 2m at along the route.

Table C.5: Direct effect of weather on shipping time – comparison between routes and ports

	route weather on route time		port weather on port time	
	(1)	(2)	(3)	(4)
average wave	0.6791***		0.6795***	
	(0.0773)		(0.1198)	
wave <0.5m		*ref*		*ref*
wave 0.5-0.8m		0.0597		0.0894
		(0.0419)		(0.1000)
wave 0.8-1.3m		0.1472**		0.3137**
		(0.0601)		(0.1432)
wave 1.3-2m		0.4616***		0.5767***
		(0.0986)		(0.2009)
wave >2m		1.2374***		1.4580***
		(0.1480)		(0.2454)
unit	route	route	port	port
date (day) FE	✓	✓	✓	✓
ship-unit FE	✓	✓	✓	✓
unit-month FE	✓	✓	✓	✓
unit-year FE	✓	✓	✓	✓
# observations	1,555,030	1,555,030	6,905,453	6,905,453
# clusters	255	255	1,664	1,664

Standard errors in parentheses

* $p < 0.10$, ** $p < 0.05$, *** $p < 0.01$

Weather at port hence seems to be only marginally more important than weather at sea. However, weather at port can influence time spent on the route, as highlighted in section C.3,

because ships tend to lower their speed (or stop) when their destination port is congested. But weather along the route seems more unlikely to influence the time spent at ports. To test these mechanisms, I consider a similar specification:

$$\text{time}_{sit} = \beta \text{ weather}_{jt} + \delta_{si} + \delta_t + \delta_{im} + \delta_{iy} + \epsilon_{sit} \tag{C.71}$$

where either i is a route, in which case j is the destination port of this route – i.e. I measure the effect of weather in the destination port on the time spend on the route (expected to be positive, as in section C.3); or i is a port, in which case j is a route arriving at port i – i.e. I investigate the effect of weather along a route on the time spent in destination port (expected to be close to null).

Table C.6: Cross effect of weather on shipping time – comparison between routes and ports

	port weather on route time		route weather on port time	
	(1)	(2)	(3)	(4)
average wave	0.9510***		0.0863	
	(0.0489)		(0.0794)	
wave <0.5m		*ref*		*ref*
wave 0.5-0.8m		0.2030***		-0.2766**
		(0.0314)		(0.1207)
wave 0.8-1.3m		0.5284***		-0.2444*
		(0.0421)		(0.1457)
wave 1.3-2m		1.0529***		-0.1409
		(0.0636)		(0.1543)
wave >2m		1.8893***		0.2233
		(0.1136)		(0.2036)
weather unit	port route	port route	route port	route port
date (day) FE	✓	✓	✓	✓
ship-unit FE	✓	✓	✓	✓
unit-month FE	✓	✓	✓	✓
unit-year FE	✓	✓	✓	✓
# observations	5,265,994	5,265,994	426,331	426,331
# clusters	13,605	13,605	101	101

Standard errors in parentheses

* $p < 0.10$, ** $p < 0.05$, *** $p < 0.01$

The results in Table C.6 show that indeed, port weather can have a significant effect on time spent along the route (columns 1 and 2), but the reverse is not true (columns 3 and 4). Hence

adverse weather conditions in a port increase significantly the shipping time, both because of higher time spent in the port and along the route ; while time at sea has a smaller effect, only along the route. This justifies focusing on the effects of weather in the ports.

D Additional estimation results

Table D.7: Effect of traffic, local weather and downstream weather on port dwell time

	log dwell time
local wave average height (MA)	0.03153***
	(0.00421)
log traffic (MA)	0.13999***
	(0.00605)
downstream wave average height (MA)	0.00002
	(0.00006)
date FE	✓
ship-port FE	✓
port-year FE	✓
# observations	6,295,439
# ships	11,371
# ports	1,357

Standard errors in parentheses

* $p < 0.10$, ** $p < 0.05$, *** $p < 0.01$

Table D.8: Effect of moving-average traffic and weather on port dwell time

	(1) no traffic	(2) OLS	(3) IV
wave average height (MA)	0.03481***	0.03257***	0.03037***
	(0.00329)	(0.00282)	(0.00262)
log traffic (MA)		0.13998***	0.24161***
		(0.00606)	(0.03519)
date FE	✓	✓	✓
ship-port FE	✓	✓	✓
port-year FE	✓	✓	✓
# observations	6,295,537	6,295,439	6,108,351
# ships	11,371	11,371	11,309
# ports	1,357	1,357	1,354
First Stage KP-F			151.2
First Stage CD-F			22818.5

Standard errors in parentheses

* $p < 0.10$, ** $p < 0.05$, *** $p < 0.01$

Table D.9: Effect of moving-average traffic and weather on port dwell time

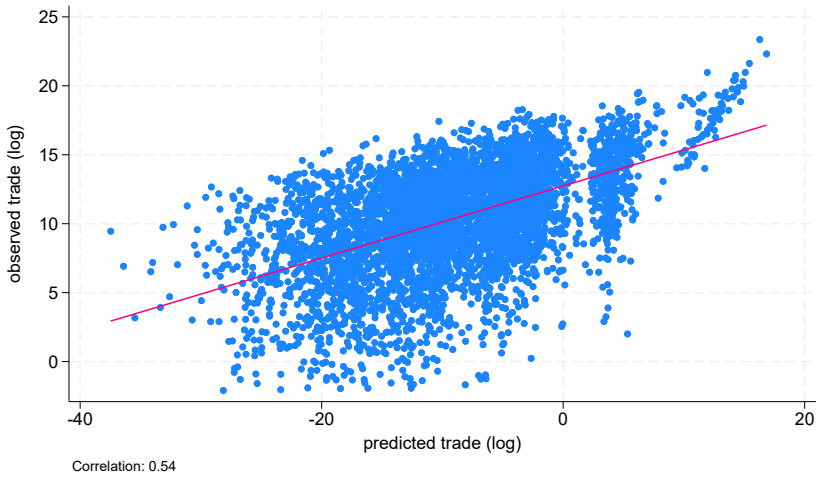
	no traffic		OLS		IV	
	(1)	(2)	(3)	(4)	(5)	(6)
wave avg (MA)	0.03509***		0.03264***		0.02463***	
	(0.00328)		(0.00273)		(0.00364)	
# days wave <p50 (MA)		*ref*		*ref*		*ref*
# days wave p50-p90 (MA)		0.00376		0.00402		0.00534
		(0.00300)		(0.00287)		(0.00354)
# days wave p90-p97 (MA)		0.01984***		0.01815**		0.00957
		(0.00767)		(0.00735)		(0.00815)
# days wave >p97 (MA)		0.07478***		0.07361***		0.06769***
		(0.00854)		(0.00753)		(0.01257)
log traffic (MA)			0.13943***	0.13977***	0.59305***	0.84359***
			(0.00580)	(0.00580)	(0.08968)	(0.10826)
date FE	✓	✓	✓	✓	✓	✓
ship-port FE	✓	✓	✓	✓	✓	✓
port-year FE	✓	✓	✓	✓	✓	✓
# observations	6,716,126	6,716,126	6,715,986	6,715,986	6,715,986	6,715,986
# ships	11,558	11,558	11,558	11,558	11,558	11,558
# ports	1,390	1,390	1,390	1,390	1,390	1,390
First Stage KP-F					12.91	12.29
First Stage CD-F					1005.2	1026.5

Standard errors in parentheses

* $p < 0.10$, ** $p < 0.05$, *** $p < 0.01$

E Test of model fit

Figure E.3: Predicted trade flows using traffic compared to observed trade flows



F Computing counterfactuals

The international trade setting requires to take into account trade deficit between locations. I follow the trade literature to handle this feature in the empirical application, in two steps.

First, given baseline $\{\Xi_{ij0}, Y_{i0}, E_{i0}\}$ observed in the data, I compute counterfactual outcomes assuming no weather shock ($\Delta\text{weather}_i = 0 \quad \forall i \in \mathcal{N}$), but deficits go to zero ($\kappa_i' = 0$, i.e. $\widehat{(1+\kappa_i)} = \frac{1}{1+\kappa_i} = \frac{Y_i}{E_i} \quad \forall i \in \mathcal{N}$). It amounts to solving the following system of equations:

$$\hat{y}_{i1}^{\frac{1+\theta}{1-\lambda\theta}} \hat{P}_{i1}^{\frac{-\theta}{1-\lambda\theta}+\theta} = \left(\frac{Y_{i0}}{E_{i0} + \sum_j \Xi_{ij0}}\right) \hat{y}_{i1} \hat{P}_{i1}^{\theta} + \sum_{j=1}^{N} \left(\frac{\Xi_{ij0}}{E_{i0} + \sum_j \Xi_{ij0}}\right) \hat{y}_{j1}^{\theta+1} \tag{F.72}$$

$$\hat{y}_{i1}^{\frac{\theta+1}{1-\lambda\theta}-(\theta+1)} \hat{P}_{i1}^{\frac{-\theta}{1-\lambda\theta}} = \left(\frac{Y_{i0}}{Y_{i0} + \sum_j \Xi_{ji0}}\right) \hat{y}_{i1}^{-\theta} + \sum_{j=1}^{N} \left(\frac{\Xi_{ji0}}{Y_{i0} + \sum_j \Xi_{ji0}}\right) \hat{P}_{j1}^{-\theta} \tag{F.73}$$

This allows to retrieve first step counterfactual levels of outcome $Y_{i1} = Y_{i0}\ \hat{y}_{i1}$ and traffic flows $\Xi_{ij1} = \Xi_{ij0}\ \hat{\Xi}_{ij1}$: those are the outcome levels if the weather profile stays the same as in the baseline period, but the trade gets balanced. By definition, we then have $Y_{i1} = E_{i1}$.

Second, given $\{\Xi_{ij1}, Y_{i1}\}$ resulted form the first step, I compute counterfactual outcomes assuming that the trade deficits stay to zero ($\kappa_i = \kappa_i' = 0$, $\widehat{(1+\kappa_i)} = 1 \quad \forall i \in \mathcal{N}$) but that weather changes ($\{\Delta\text{weather}_i\}_{i\in\mathcal{N}}$). It amounts to solving the following system of equations:

$$\hat{y}_{i2}^{\frac{1+\theta}{1-\lambda\theta}} \hat{P}_{i2}^{\frac{-\theta}{1-\lambda\theta}+\theta} = \left(\frac{Y_{i1}}{E_{i1}+\sum_j \Xi_{ij1}}\right) e^{\frac{-\mu\theta}{1-\lambda\theta}\Delta\text{weather}_i} \hat{y}_{i2}\hat{P}_{i2}^{\theta} + \sum_{j=1}^{N}\left(\frac{\Xi_{ij1}}{Y_{i1}+\sum_j \Xi_{ij1}}\right) e^{\frac{-\mu\theta}{1-\lambda\theta}\Delta\text{weather}_i} \hat{y}_{j2}^{\theta+1} \tag{F.74}$$

$$\hat{y}_{i2}^{\frac{\theta+1}{1-\lambda\theta}-(\theta+1)} \hat{P}_{i2}^{\frac{-\theta}{1-\lambda\theta}} = \left(\frac{Y_{i1}}{Y_{i1}+\sum_j \Xi_{ji1}}\right) e^{\frac{-\mu\theta}{1-\lambda\theta}\Delta\text{weather}_i} \hat{y}_{i2}^{-\theta} + \sum_{j=1}^{N}\left(\frac{\Xi_{ji1}}{Y_{i1}+\sum_j \Xi_{ji1}}\right) e^{\frac{-\mu\theta}{1-\lambda\theta}\Delta\text{weather}_i} \hat{P}_{j2}^{-\theta} \tag{F.75}$$

I compute the treatment effect of the change in weather as the difference between equilibrium levels in the two counterfactuals, i.e. nominal outcome changes $\hat{y}_{i2}$ and real outcome changes $\hat{y}_{i2}/\hat{P}_{i2}$.

This method is standard in international trade literature to address deficits (Ossa, 2016). An alternative approach would be to compute just one counterfactual holding the deficits fixed relative to the observed equilibrium; however, this method causes convergence issues.

G Algorithm for conducting counterfactuals

I adapt the algorithm of Allen & Arkolakis (2022) to find the equilibrium in our counterfactual simulations. It consists of a loop solving for vectors of $\{\hat{y}_i\}$ and $\{\hat{P}_i\}$. Equilibrium equations 33 and 34 form a system of non-linear equations in $\{\hat{y}_i\}$ and $\{\hat{P}_i\}$. At the same time, the term on the left-hand side of each of the equilibrium conditions is a log-linear combination of the endogenous variables.

I start with an initial guess of the endogenous variables $\{\hat{y}_i\}_{(0)} = 1$ and $\{\hat{P}_i\}_{(0)} = 1$ and plug it into the equilibrium conditions 33 and 34. To help us update the guess, I define the following:

$$\hat{x}_{1,i} \equiv \hat{y}_i^{\theta+1+\frac{\lambda\theta(\theta+1)}{1-\lambda\theta}} \hat{P}_i^{-\frac{\lambda\theta^2}{1-\lambda\theta}}$$

$$\hat{x}_{2,i} \equiv \hat{y}_i^{\frac{\lambda\theta(\theta+1)}{1-\lambda\theta}} \hat{P}_i^{-\theta-\frac{\lambda\theta^2}{1-\lambda\theta}}$$

so that:

$$\begin{pmatrix} \ln \hat{x}_{1,i} \\ \ln \hat{x}_{2,i} \end{pmatrix} = \begin{pmatrix} \theta + 1 + \frac{\lambda\theta(\theta+1)}{1-\lambda\theta} & -\frac{\lambda\theta^2}{1-\lambda\theta} \\ \frac{\lambda\theta(\theta+1)}{1-\lambda\theta} & -\theta - \frac{\lambda\theta^2}{1-\lambda\theta} \end{pmatrix} \begin{pmatrix} \ln \hat{y}_i \\ \ln \hat{P}_i \end{pmatrix} \iff$$

$$\begin{pmatrix} \ln \hat{y}_i \\ \ln \hat{P}_i \end{pmatrix} = \begin{pmatrix} \theta + 1 + \frac{\lambda\theta(\theta+1)}{1-\lambda\theta} & -\frac{\lambda\theta^2}{1-\lambda\theta} \\ \frac{\lambda\theta(\theta+1)}{1-\lambda\theta} & -\theta - \frac{\lambda\theta^2}{1-\lambda\theta} \end{pmatrix}^{-1} \begin{pmatrix} \ln \hat{x}_{1,i} \\ \ln \hat{x}_{2,i} \end{pmatrix}$$

By this definition, for a guess of $\left(\{\hat{y}_i\}_{(0)}, \{\hat{P}_i\}_{(0)}\right)$, the equilibrium conditions yield a set of vectors $\left(\{\hat{x}_{1,i}\}_{(1)}, \{\hat{x}_{2,i}\}_{(1)}\right)$, which by the log-linear transformation defined above, imply an updated guess of $\left(\{\hat{y}_i\}_{(1)}, \{\hat{P}_i\}_{(1)}\right)$. On each iteration, I rescale the vectors $\left(\{\hat{x}_{1,i}\}_{(1)}, \{\hat{x}_{2,i}\}_{(1)}\right)$ such that the second period income distribution still sums to 1, and update the guess of $\left(\{\hat{y}_i\}_{(0)}, \{\hat{P}_i\}_{(0)}\right)$ towards $\left(\{\hat{x}_{1,i}\}_{(1)}, \{\hat{x}_{2,i}\}_{(1)}\right)$. I iterate through this procedure until the equilibrium conditions are solved. Therefore, this loop returns a $\left(\{\hat{y}_i\}_{(0)}, \{\hat{P}_i\}_{(0)}\right)$ for which:[31]

$$(\hat{x}_{1,i})_{(1)} = \left(\frac{E_i}{E_i + \sum_j \Xi_{ij}}\right) e^{\frac{-\mu\theta}{1-\lambda\theta}\Delta\text{weather}_i} (\hat{y}_i)_{(0)} (\hat{P}_i)^{\theta}_{(0)} + \sum_{j=1}^{N} \left(\frac{\Xi_{ij}}{E_i + \sum_j \Xi_{ij}}\right) e^{\frac{-\mu\theta}{1-\lambda\theta}\Delta\text{weather}_i} (\hat{y}_j)^{\theta+1}_{(0)}$$

$$(\hat{x}_{2,i})_{(1)} = \left(\frac{Y_i}{Y_i + \sum_j \Xi_{ji}}\right) e^{\frac{-\mu\theta}{1-\lambda\theta}\Delta\text{weather}_i} (\hat{y}_i)^{-\theta}_{(0)} + \sum_{j=1}^{N} \left(\frac{\Xi_{ji}}{Y_i + \sum_j \Xi_{ji}}\right) e^{\frac{-\mu\theta}{1-\lambda\theta}\Delta\text{weather}_i} (\hat{P}_j)^{-\theta}_{(0)}$$

[31] This system assumes a constant deficit ratio κ; however the system can be adapted straightforwardly to consider rather a change in trade deficit, as done in the first step of Section F.

H Additional counterfactual results

Figure H.4: Changes in nominal outcome at the port catchment area level when increasing wave height in Singapore

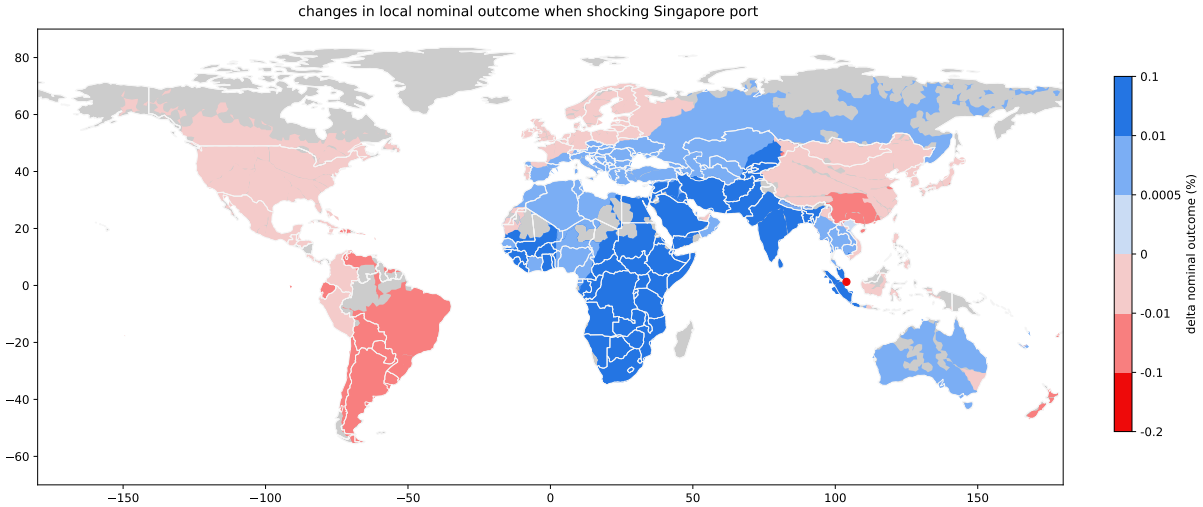


Figure H.5: Changes in nominal outcome at the country level when increasing wave height in Singapore

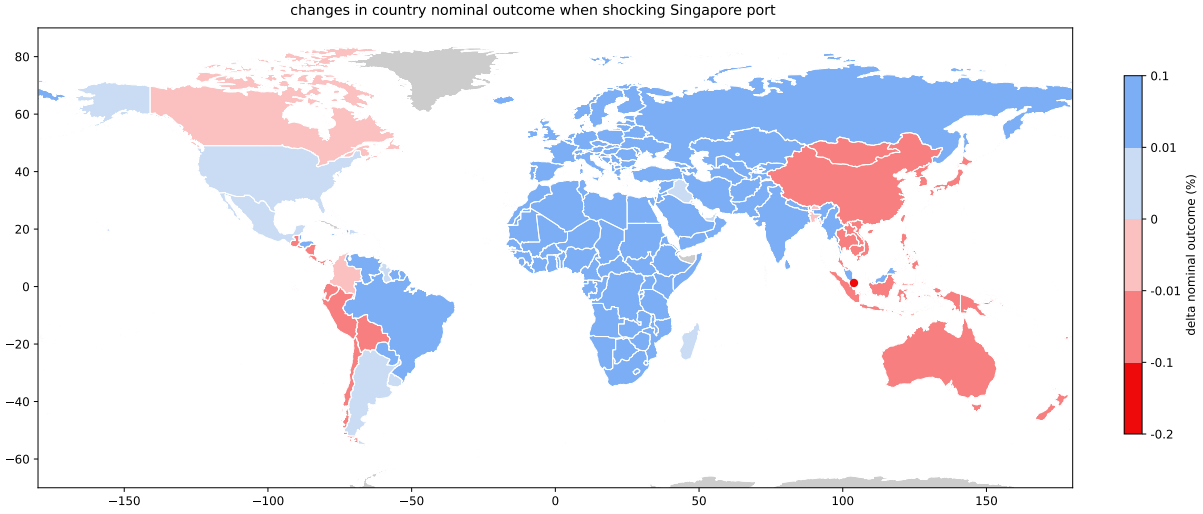


Figure H.6: Average changes in real outcome at the country level when increasing wave height in Singapore

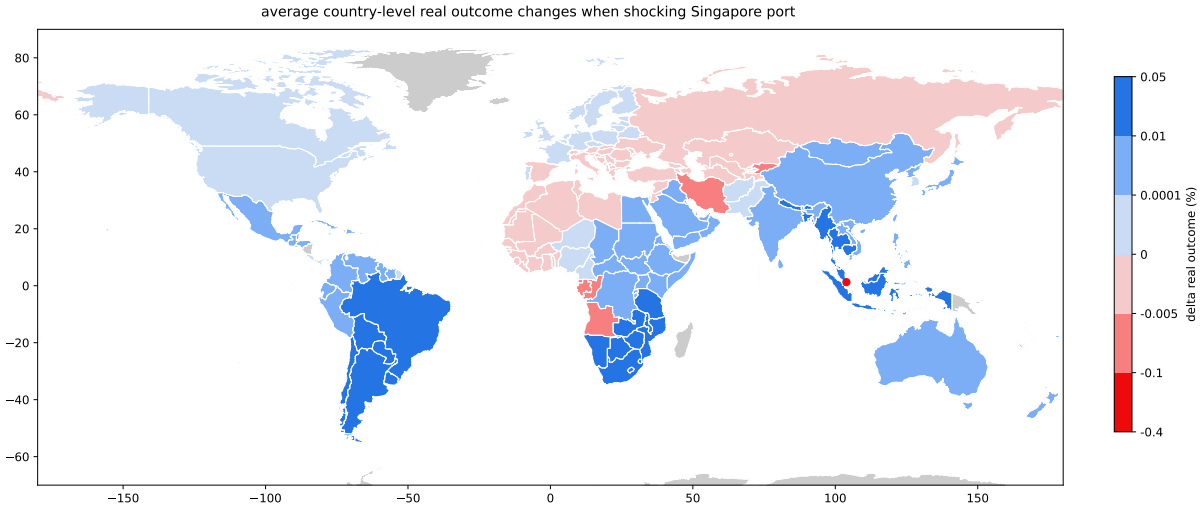


Figure H.7: Change is global nominal outcome when increasing wave height in each port

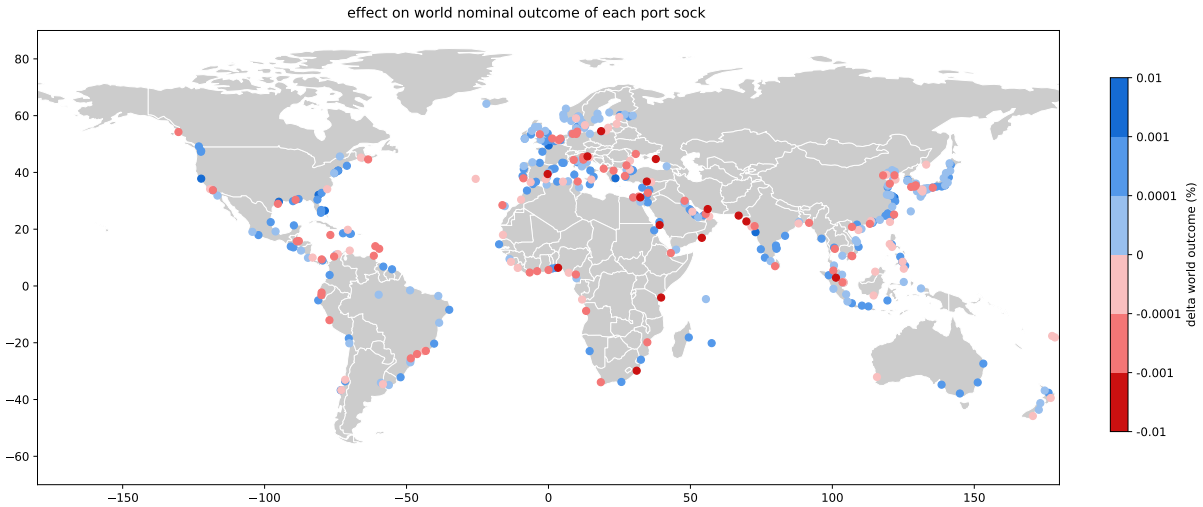


Figure H.8: Nominal outcome-weighted global real outcome changes when increasing wave height in each port

